Magnetic Properties and Superconductivity

Session: 2022-2023
Course code: PHY 3101
Course title: Electrical Engineering Materials
Bachelor of Science in Electrical and Electronic Engineering
Jashore University of Science and Technology

Content

Magnetic properties of materials, Magnetic moment, magnetization and relative permitivity, different types of magnetic materials, origin of ferromagnetism and magnetic domains. Introduction to superconductivity, Zero resistance and Meissner effect, Type I and Type II superconductors and critical current density.

References

Principles of electronic materials and devices – S. O. Kasap
Electrical Engineering Materials – A. J. Dekker
Superconductivity: Basics and Applications to Magnets – R.G. Sharma

CHAPTER

8

Magnetic Properties and Superconductivity

Many electrical engineering devices such as inductors, transformers, rotating machines, and ferrite antennas are based on utilizing the magnetic properties of materials. There are many instances where permanent magnets are also used either on their own or as part of a device such as a rotating machine or a loud speaker. The majority of engineering devices make use of the ferromagnetic and ferrimagnetic properties, which are therefore treated in much more detail than other magnetic properties such as diamagnetism and paramagnetism. Although superconductivity involves the vanishing of the resistivity of a conductor at low temperatures and is normally explained within quantum mechanics, we treat the subject in this chapter because all superconductors are perfect diamagnets and, further, they have present or potential uses that involve magnetic fields. The advent of high-T_c superconductivity, discovered in 1986 by George Bednorz and Alex Müller at IBM Research Laboratories in Zürich, is undoubtedly one of the most significant discoveries over the last 50 years, as popularized in various magazines. High-T_c superconductors are already finding applications in such devices as superconducting solenoids, sensitive magnetometers, and high-Q microwave filters.

8.1 MAGNETIZATION OF MATTER

8.1.1 MAGNETIC DIPOLE MOMENT

Magnetic properties of materials involve concepts based on the magnetic dipole moment. Consider a current loop, as shown in Figure 8.1, where the circulating current is I. This may, for example, be a coil carrying a current. For simplicity we will assume that the current loop lies within a single plane. The area enclosed by the current is A. Suppose that $\mathbf{u}_n$ is a unit vector coming out from the area A. The direction of $\mathbf{u}_n$ is such that

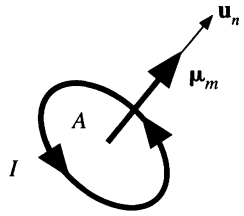

Figure 8.1 Definition of a magnetic dipole moment.

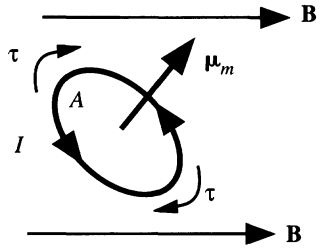

Figure 8.2 A magnetic dipole moment in an external field experiences a torque.

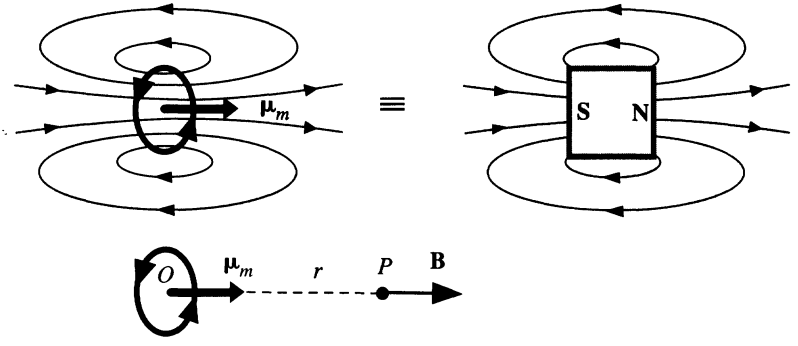

Figure 8.3 A magnetic dipole moment creates a magnetic field just like a bar magnet.
The field **B** depends on μ_m.

looking along it, the current circulates clockwise. Then the **magnetic dipole moment,** or simply the **magnetic moment** $\boldsymbol{\mu}_m$, is defined by[1]

Definition of magnetic moment

$$\boldsymbol{\mu}_m = IA\mathbf{u}_n \qquad [8.1]$$

When a magnetic moment is placed in a magnetic field, it experiences a torque that tries to rotate the magnetic moment to align its axis with the magnetic field, as depicted in Figure 8.2. Moreover, since a magnetic moment is a current loop, it gives rise to a magnetic field **B** around it, as shown in Figure 8.3, which is similar to the magnetic field around a bar magnet. We can find the field **B** from the current I and its geometry, which are treated in various physics textbooks. For example, the field **B** at a point P at a distance r along the axis of the coil from the center, as shown in Figure 8.3, is directly proportional to the magnitude of the magnetic moment but inversely proportional to r^3, that is, $\mathbf{B} \propto \boldsymbol{\mu}_m / r^3$.

[1] The symbol $\boldsymbol{\mu}$ for the magnetic dipole moment should not be confused with the permeability. Absolute and relative permeabilities will be denoted by μ_o and μ_r.

8.1.2 ATOMIC MAGNETIC MOMENTS

An orbiting electron in an atom behaves much like a current loop and has a magnetic dipole moment associated with it, called the **orbital magnetic moment** (μ_{orb}), as illustrated in Figure 8.4. If ω is the angular frequency of the electron, then the current I due to the orbiting electron is

$$I = \text{Charge flowing per unit time} = -\frac{e}{\text{Period}} = -\frac{e\omega}{2\pi}$$

If r is the radius of the orbit, then the magnetic dipole moment is

$$\mu_{orb} = I(\pi r^2) = -\frac{e\omega r^2}{2}$$

But the velocity v of the electron is ωr and its orbital angular momentum is

$$L = (m_e v)r = m_e \omega r^2$$

Using this in μ_{orb}, we get

$$\mu_{orb} = -\frac{e}{2m_e}L \qquad [8.2]$$

Orbital magnetic moment of the electron

We see that the magnetic moment is proportional to the orbital angular momentum through a factor that has the charge to mass ratio of the electron. The numerical factor, in this case $e/2m_e$, relating the angular momentum to the magnetic moment, is called the **gyromagnetic ratio.** The negative sign in Equation 8.2 indicates that μ_{orb} is in the opposite direction to L and is due to the negative charge of the electron.

The electron also has an intrinsic angular momentum S, that is, spin. The spin of the electron has a **spin magnetic moment,** denoted by μ_{spin}, but the relationship between μ_{spin} and S is not the same as that in Equation 8.2. The gyromagnetic ratio is a factor of 2 greater,

$$\mu_{spin} = -\frac{e}{m_e}S \qquad [8.3]$$

Spin magnetic moment of the electron

The overall magnetic moment of the electron consists of $\boldsymbol{\mu}_{orb}$ and $\boldsymbol{\mu}_{spin}$ appropriately added. We cannot simply add them numerically as they are vector quantities. Furthermore, the overall magnetic moment $\boldsymbol{\mu}_{atom}$ of the atom itself depends on the

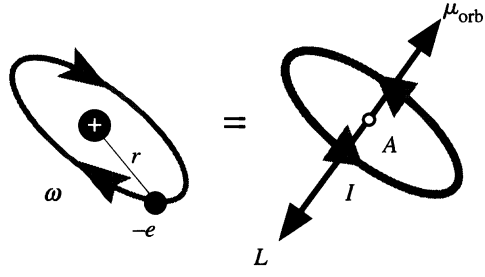

Figure 8.4 An orbiting electron is equivalent to a magnetic dipole moment μ_{orb}.

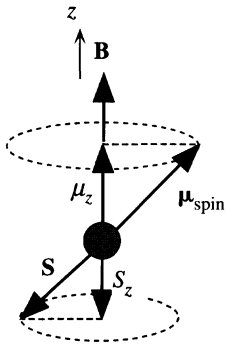

Figure 8.5 The spin magnetic moment precesses about an external magnetic field along z and has a value μ_z along z.

orbital motions and spins of *all* the electrons. Electrons in closed subshells, however, do not contribute to the overall magnetic moment because for every electron with a given **L** (or **S**), there is another one with an opposite **L** (or **S**). The reason is that the direction of **L** is space quantized by m_ℓ and all negative and positive values of m_ℓ are occupied in a closed shell. Similarly, there are as many electrons spinning up as there are spinning down, so there is no net electron spin in a closed shell and no net $\boldsymbol{\mu}_{spin}$. Thus, only **unfilled subshells** contribute to the overall magnetic moment of an atom.

Consider an atom that has closed inner shells and a single electron in an s orbital ($\ell = 0$). This means that the orbital magnetic moment is zero and the atom has a magnetic moment due to the spin of the electron alone, $\boldsymbol{\mu}_{atom} = \boldsymbol{\mu}_{spin}$. In the presence of an external magnetic field along the z direction, the magnetic moment cannot simply rotate and align with the field because quantum mechanics requires the spin angular momentum to be space quantized, that is, S_z (the component of **S** along z) must be $m_s\hbar$ where $m_s = \pm\frac{1}{2}$ is the spin magnetic quantum number. The torque experienced by the spinning electron causes the spin magnetic moment to precess about the external magnetic field, as shown in Figure 8.5. This precession is such that $S_z = -\frac{1}{2}\hbar$ and leads to an average magnetic moment μ_z along the field given by Equation 8.3 with S_z, that is,

Magnetic moment along the field

$$\mu_z = -\frac{e}{m_e}S_z = -\frac{e}{m_e}(m_s\hbar) = \frac{e\hbar}{2m_e} = \beta \qquad [8.4]$$

The quantity $\beta = e\hbar/2m_e$ is called the **Bohr magneton** and has the value 9.27×10^{-24} A m^2 or J T^{-1}.

Thus, the spin of a single electron has a magnetic moment of one Bohr magneton along the field.

8.1.3 MAGNETIZATION VECTOR M

Consider a tightly wound long solenoid, ideally infinitely long, with free space (or vacuum) as the medium inside the solenoid, as shown in Figure 8.6a. The magnetic field inside the solenoid is denoted by $\mathbf{B}_o$ to specifically identify this field as in free space.

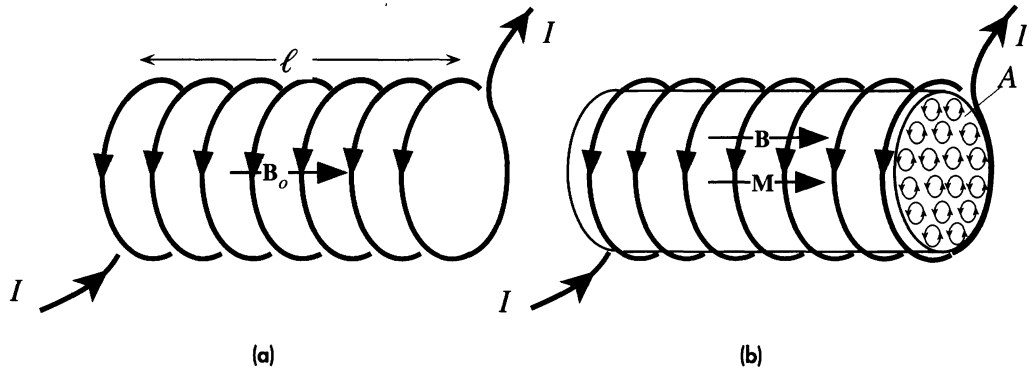

Figure 8.6
(a) Consider a long solenoid. With free space as the medium inside, the magnetic field is $\mathbf{B}_o$.
(b) A material medium inserted into the solenoid develops a magnetization **M**.

This field depends on the current I through the solenoid wire and the number of turns per unit length n and is given by[2]

$$B_o = \mu_o n I = \mu_o I' \qquad [8.5]$$

Free space field inside solenoid

where I' is the current per unit length of the solenoid, that is, $I' = nI$, and μ_o is the absolute permeability of free space in henries per meter, H m^{-1}.

If we now place a cylindrical material medium to fill the inside of this solenoid, as in Figure 8.6b, we find that the magnetic field has changed. The new magnetic field in the presence of a medium is denoted as **B**. We will take $\mathbf{B}_o$ to be the applied magnetic field into which the material medium is placed.

Each atom of the material responds to the applied field $\mathbf{B}_o$ and develops, or acquires, a net magnetic moment $\boldsymbol{\mu}_m$ along the applied field. We can view each magnetic moment $\boldsymbol{\mu}_m$ as the result of the precession of each atomic magnetic moment about $\mathbf{B}_o$. The medium therefore develops a net magnetic moment along the field and becomes **magnetized.** The magnetic vector **M** describes the extent of magnetization of the medium. **M** is defined as the **magnetic dipole moment per unit volume.** Suppose that there are N atoms in a small volume ΔV and each atom i has a magnetic moment $\boldsymbol{\mu}_{mi}$ (where $i = 1$ to N). Then **M** is defined by

$$\mathbf{M} = \frac{1}{\Delta V}\sum_{i=1}^{N} \boldsymbol{\mu}_{mi} = n_{\text{at}}\boldsymbol{\mu}_{\text{av}} \qquad [8.6]$$

Magnetization vector

where n_{at} is the number of atoms per unit volume and $\boldsymbol{\mu}_{\text{av}}$ is the average magnetic moment per atom. We can assume that each atom acquires a magnetic moment $\boldsymbol{\mu}_{\text{av}}$ along $\mathbf{B}_o$. Each of these magnetic moments along $\mathbf{B}_o$ can be viewed as an elementary current loop at the atomic scale, as schematically depicted in Figure 8.6b. These elementary

[2] The proof of this comes out from Ampere's law and can be found in any textbook of electromagnetism.

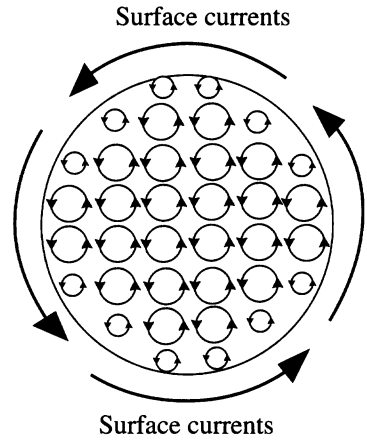

Figure 8.7 Elementary current loops result in surface currents.
There is no internal current, as adjacent currents on neighboring loops are in opposite directions.

current loops are due to electronic currents within the atom and arise from both orbital and spin motions of the electrons. Each current loop has its current plane normal to $\mathbf{B}_o$.

Consider a cross section of the magnetized medium, as in Figure 8.7. All the elementary current loops in this plane have the current circulation in the same direction inasmuch as each atom acquires the same magnetic moment $\boldsymbol{\mu}_{av}$. All neighboring loops in the bulk have adjacent currents in opposite directions that cancel each other, as apparent in Figure 8.7. Thus, there are no net bulk currents, or internal currents, within the bulk of the material. However, the currents at the surface in the surface loops cannot be canceled and this leads to a net **surface current,** as depicted in Figure 8.7. The surface currents are induced by the magnetization of the medium by the applied magnetic field and therefore depend on the magnetization M of the specimen.

From the definition of M, the total magnetic moment of the cylindrical specimen is

$$\text{Total magnetic moment} = M\,(\text{Volume}) = MA\ell$$

Suppose that the magnetization current on the surface per unit length of the specimen is I_m. Then the total circulating surface current is $I_m\ell$ and the total magnetic moment of the specimen, by definition, is

$$\text{Total magnetic moment} = (\text{Total current}) \times (\text{Cross-sectional area}) = I_m\ell A$$

Magnetization and surface currents

Equating the two total magnetic moments, we find

$$M = I_m \qquad [8.7]$$

We derived this for a particular sample geometry, a cylindrical specimen, in which **M** is along the axis of the cylindrical specimen and I_m flows in a plane perpendicular to **M**. The relationship, however, is more general, as derived in more advanced texts. It should be emphasized that the magnetization current I_m is not due to the flow of free charge carriers, as in a current-carrying copper wire, but due to localized electronic currents within the atoms of the solid at the surface. Equation 8.7 states that we can represent the magnetization of a medium by a surface current per unit length I_m that is equal to M.

8.1.4 MAGNETIZING FIELD OR MAGNETIC FIELD INTENSITY H

The magnetized specimen in Figure 8.6b placed inside the solenoid develops magnetization currents on the surface. It therefore behaves like a solenoid. We can now regard the solenoid with medium inside, as depicted in Figure 8.8. The magnetic field within the medium now arises from not only the conduction current per unit length I' in the solenoid wires but also from the magnetization current I_m on the surface. The magnetic field B inside the solenoid is now given by the usual solenoid expression but with a current that includes both I' and I_m, as shown in Figure 8.8:

$$B = \mu_o(I' + I_m) = B_o + \mu_o M$$

This relationship is generally valid and can be written in vector form as

Magnetic field in a magnetized medium

$$\mathbf{B} = \mathbf{B}_o + \mu_o \mathbf{M} \qquad [8.8]$$

The field at a point inside a magnetized material is the sum of the applied field $\mathbf{B}_o$ and a contribution from the magnetization $\mathbf{M}$ of the material. The magnetization arises from the application of $\mathbf{B}_o$ due to the current of free carriers in the solenoid wires, called the **conduction current,** which we can externally adjust. It becomes useful to introduce a vector field that represents the effect of the external or conduction current alone. In general, $\mathbf{B} - \mu_o\mathbf{M}$ at a point is the contribution of the external currents alone to the magnetic field at that point inside the material that we called $\mathbf{B}_o$. $\mathbf{B} - \mu_o\mathbf{M}$ represents a magnetizing field because it is the field of the external currents that magnetize the material. The **magnetizing field H** is defined as

Definition of the magnetizing field

$$\mathbf{H} = \frac{1}{\mu_o}\mathbf{B} - \mathbf{M} \qquad [8.9]$$

or

Definition of the magnetizing field

$$\mathbf{H} = \frac{1}{\mu_o}\mathbf{B}_o$$

The magnetizing field is also known as the **magnetic field intensity** and is measured in A m^{-1}. The reason for the division by μ_o is that the resulting vector field $\mathbf{H}$ becomes simply related to the external conduction currents (through Ampere's law). Since in the solenoid $\mathbf{B}_o$ is $\mu_o n I$, we see that the magnetizing field in a solenoid is

$$H = nI = \text{Total conduction current per unit length} \qquad [8.10]$$

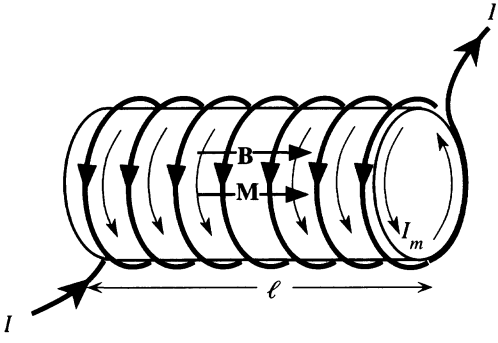

Figure 8.8 The field **B** in the material inside the solenoid is due to the conduction current I through the wires and the magnetization current I_m on the surface of the magnetized medium, or $\mathbf{B} = \mathbf{B}_o + \mu_o\mathbf{M}$.

It is generally helpful to imagine **H** as the *cause* and **B** as the *effect.* The cause **H** depends only on the external conduction currents, whereas the effect **B** depends on the magnetization **M** of matter.

8.1.5 MAGNETIC PERMEABILITY AND MAGNETIC SUSCEPTIBILITY

Suppose that at a point P in a material, the magnetic field is **B** and the magnetizing field is **H**. We let $\mathbf{B}_o$ be the magnetic field at P in the absence of any material (*i.e.*, in free space). The magnetic permeability of the medium at P is defined as the magnetic field per unit magnetizing field,

Definition of magnetic permeability

$$\mu = \frac{B}{H} \qquad [8.11]$$

It relates the effect B to the cause H at the same point P inside a material. In simple qualitative terms, μ represents to what extent a medium is permeable by magnetic fields. Relative permeability μ_r of a medium is the fractional increase in the magnetic field with respect to the field in free space when a material medium is introduced. For example, suppose that the field in a solenoid with free space in it is B_o but with material inserted it is B. Then μ_r is defined by

Definition of relative permeability

$$\mu_r = \frac{B}{B_o} = \frac{B}{\mu_o H} \qquad [8.12]$$

From Equations 8.11 and 8.12, clearly,

$$\mu = \mu_o \mu_r$$

The magnetization **M** produced in a material depends on the net magnetic field **B**. It would be natural to proceed as in dielectrics by relating **M** to **B** analogously to relating P (polarization) to $\mathcal{E}$ (electric field). However, for historic reasons, **M** is related to **H**, the magnetizing field. Suppose that the medium is isotropic (same properties in all directions), then magnetic susceptibility χ_m of the medium is defined simply by

Definition of magnetic susceptibility

$$\mathbf{M} = \chi_m \mathbf{H} \qquad [8.13]$$

This relationship is not obeyed by all magnetic materials. For example, as we will see later, ferromagnetic materials do not obey Equation 8.12. Since the magnetic field

$$\mathbf{B} = \mu_o(\mathbf{H} + \mathbf{M})$$

we have

$$B = \mu_o H + \mu_o M = \mu_o H + \mu_o \chi_m H = \mu_o(1 + \chi_m)H$$

and

Relative permeability and susceptibility

$$\mu_r = 1 + \chi_m \qquad [8.14]$$

The presence of a magnetizable material is conveniently accounted for by using the relative permeability μ_r, or $(1 + \chi_m)$, to simply multiply μ_o. Alternatively, one can simply replace μ_o with $\mu = \mu_o \mu_r$. For example, the inductance of the solenoid with a magnetic medium inside increases by a factor of μ_r.

Table 8.1 provides a summary of various important magnetic quantities, their definitions, and units.

Table 8.1 Magnetic quantities and their units

Magnetic Quantity	Symbol	Definition	Units	Comment
Magnetic field; magnetic induction	$\mathbf{B}$	$\mathbf{F} = q\mathbf{v} \times \mathbf{B}$	T = tesla = webers m^{-2}	Produced by moving charges or currents, acts on moving charges or currents.
Magnetic flux	Φ	$\Delta\Phi = B_{\text{normal}}\,\Delta A$	Wb = weber	$\Delta\Phi$ is flux through ΔA and B_{normal} is normal to ΔA. Total flux through any closed surface is zero.
Magnetic dipole moment	$\boldsymbol{\mu}_m$	$\mu_m = IA$	A m^2	Experiences a torque in $\mathbf{B}$ and a net force in a nonuniform $\mathbf{B}$.
Bohr magneton	β	$\beta = e\hbar/2m_e$	A m^2 or J T^{-1}	Magnetic moment due to the spin of the electron. $\beta = 9.27 \times 10^{-24}$ A m^2
Magnetization vector	$\mathbf{M}$	Magnetic moment per unit volume	A m^{-1}	Net magnetic moment in a material per unit volume.
Magnetizing field; magnetic field intensity	$\mathbf{H}$	$\mathbf{H} = \mathbf{B}/\mu_o - \mathbf{M}$	A m^{-1}	$\mathbf{H}$ is due to external conduction currents only and is the cause of $\mathbf{B}$ in a material.
Magnetic susceptibility	χ_m	$\mathbf{M} = \chi_m\mathbf{H}$	None	Relates the magnetization of a material to the magnetizing field $\mathbf{H}$.
Absolute permeability	μ_o	$c = [\varepsilon_o\mu_o]^{-1/2}$	H m^{-1} = Wb m^{-1} A^{-1}	A fundamental constant in magnetism. In free space, $\mu_o = B/H$.
Relative permeability	μ_r	$\mu_r = B/\mu_o H$	None	
Magnetic permeability	μ	$\mu = \mu_o\mu_r$	H m^{-1}	Not to be confused with magnetic moment.
Inductance	L	$L = \Phi_{\text{total}}/I$	H (henries)	Total flux threaded per unit current.
Magnetostatic energy density	E_{vol}	$dE_{\text{vol}} = H\,dB$	J m^{-3}	dE_{vol} is the energy required per unit volume in changing B by dB.

EXAMPLE 8.1

AMPERE'S LAW AND THE INDUCTANCE OF A TOROIDAL COIL Ampere's law provides a relationship between the conduction current I and the magnetic field intensity H threading this current. The conduction current I is the current due to the flow of free charge carriers through a conductor and not due to the magnetization of any medium. Consider an arbitrary closed path C around a conductor carrying a current I, as shown in Figure 8.9. The tangential component of $\mathbf{H}$ to the curve C at point P is H_t. If dl is an infinitesimally small path length of C at P, as shown in Figure 8.9, then the summation of $H_t\,dl$ around the path C gives the conduction current enclosed within C. This is **Ampere's law,**

$$\oint_C H_t\,dl = I \qquad [8.15]$$ *Ampere's law*

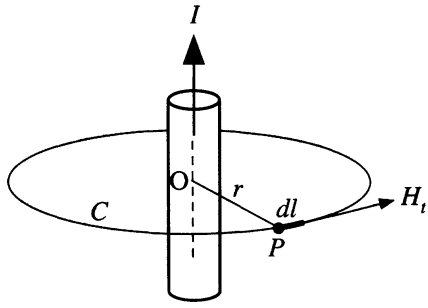

Figure 8.9 Ampere's circuital law.

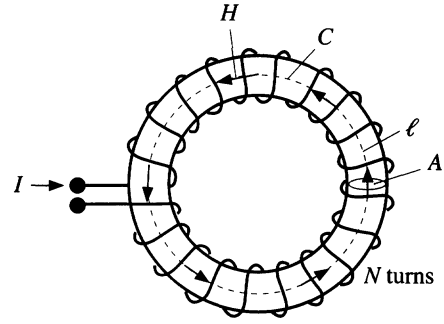

Figure 8.10 A toroidal coil with N turns.

Consider the toroidal coil with N turns shown in Figure 8.10. First assume that the toroid core is air ($\mu_r \approx 1$). Suppose that the current through the coils is I. By symmetry, the magnetic field intensity H inside the toroidal core is the same everywhere and is directed along the circumference. Suppose that l is the length of the mean circumference C. The current is linked N times by the circumference C, so Equation 8.15 is

$$\oint_C H_t \, dl = H\ell = NI$$

or

$$H = \frac{NI}{\ell}$$

The magnetic field B_o with air as core material is then simply

$$B_o = \mu_o H = \frac{\mu_o NI}{\ell}$$

When the toroidal coil has a magnetic medium with a relative permeability μ_r, the magnetic field intensity is still H because the conduction current I has not changed. But the magnetic field B is now different than B_o and is given by

Magnetic field inside toroidal coil

$$B = \mu_o \mu_r H = \frac{\mu_o \mu_r NI}{\ell}$$

If A is the cross-sectional area of the toroid, then the total flux Φ through the core is BA or $\mu_o \mu_r NAI/\ell$. The current I in Figure 8.10 threads the flux N times. The inductance L of the toroidal coil, by definition, is then

Inductance of toroidal coil

$$L = \frac{\text{Total flux threaded}}{\text{Current}} = \frac{N\Phi}{I} = \frac{\mu_o \mu_r N^2 A}{\ell}$$

Having a magnetic material as the toroid core increases the inductance by a factor of μ_r in the same way a dielectric material increases the capacitance by a factor of ε_r.

EXAMPLE 8.2 **MAGNETOSTATIC ENERGY PER UNIT VOLUME** Consider a toroidal coil with N turns that is energized from a voltage supply through a rheostat, as shown in Figure 8.11. The core of the toroid may be any material. Suppose that by adjusting the rheostat we increase the current i

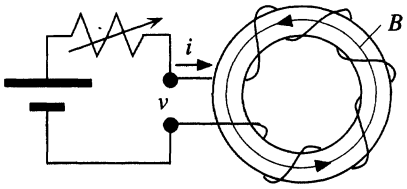

Figure 8.11 Energy required to magnetize a toroidal coil.

supplied to the coil. The current i produces magnetic flux Φ in the core, which is BA, where B is the magnetic field and A is the cross-sectional area. We can now use Ampere's law for H to relate the current i to H, as in Example 8.1. If ℓ is the mean circumference, then

$$H\ell = Ni \qquad [8.16]$$

The changing current means that the flux is also changing (both increasing). We know from Faraday's law that a changing flux that threads a circuit generates a voltage v in that circuit given by the rate of change of total threaded flux, or $N\Phi$. Lenz's law makes the polarity of the induced voltage oppose the applied voltage. Suppose that in a time interval δt seconds, the magnetic field within the core changes by δB; then $\delta\Phi = A\delta B$ and

$$v = \frac{\delta(\text{Total flux threaded})}{\delta t} = \frac{N\delta\Phi}{\delta t} = NA\frac{\delta B}{\delta t} \qquad [8.17]$$

The battery has to supply the current i against this induced voltage v, which means that it has to do electrical work iv every second. In other words, the battery has to do work $iv\,\delta t$ in a time interval δt to supply the necessary current to increase the magnetic field by δB. The electric energy δE that is input into the coil in time δt is then, using Equations 8.16 and 8.17,

$$\delta E = iv\,\delta t = \left(\frac{H\ell}{N}\right)\left(NA\frac{\delta B}{\delta t}\right)\delta t = (A\ell)H\,\delta B$$

This energy δE is the work done in increasing the field in the core by δB. The volume of the toroid is $A\ell$. Therefore, the total energy or work required per unit volume to increase the magnetic field from an initial value B_1 to a final value B_2 in the toroid is

Work done per unit volume during magnetization

$$E_{\text{vol}} = \int_{B_1}^{B_2} H\,dB \qquad [8.18]$$

where the integration limits are determined by the initial and final magnetic field. This is the expression for calculating the **energy density** (energy per unit volume) required to change the field from B_1 to B_2. It should be emphasized that Equation 8.18 is valid for *any medium*. We conclude that an incremental energy density of $dE_{\text{vol}} = H\,dB$ is required to increase the magnetic field by dB at a point in any medium including free space.

We can now consider a core material that we can represent by a *constant* relative permeability μ_r. This means we can exclude those materials that do not have a linear relationship between B and H, such as ferromagnetic and ferrimagnetic materials, which we will discuss later. If the core is free space or air, then $\mu_r = 1$.

Suppose that we increase the current in Figure 8.11 from zero to some final value I so that the magnetic field changes from zero to some final value B. Since the medium has a constant relative permeability μ_r, we can write

$$B = \mu_r\mu_o H$$

and use this in Equation 8.18 to integrate and find the energy per unit volume needed to establish the field B or field intensity H

Energy density of a magnetic field

$$E_{\text{vol}} = \frac{1}{2}\mu_r\mu_o H^2 = \frac{B^2}{2\mu_r\mu_o} \qquad [8.19]$$

This is the energy absorbed from the battery per unit volume of core medium to establish the magnetic field. This energy is stored in the magnetic field and is called **magnetostatic energy density.** It is a form of magnetic potential energy. If we were to suddenly remove the battery and short those terminals, the current will continue to flow for a short while (determined by L/R) and do external work in heating the resistor. This external work comes from the stored energy in the magnetic field. If the medium is free space, or air, then the energy density is

Magnetostatic energy density in free space

$$E_{\text{vol}}(\text{air}) = \frac{1}{2}\mu_o H^2 = \frac{B^2}{2\mu_o}$$

A magnetic field of 2 T corresponds to a magnetostatic energy density of 1.6 MJ m^{-3} or 1.6 J cm^{-3}. The energy in a magnetic field of 2 T in a 1 cm^3 volume (size of a thimble) has the work ability (potential energy) to raise an average-sized apple by 5 feet. We should note that as long as the core material is linear, that is, μ_r is independent of the magnetic field itself, magnetostatic energy density can also be written as

Magnetostatic energy in a linear magnetic medium

$$E_{\text{vol}} = \frac{1}{2}HB \qquad [8.20]$$

8.2 MAGNETIC MATERIAL CLASSIFICATIONS

In general, magnetic materials are classified into five distinct groups: diamagnetic, paramagnetic, ferromagnetic, antiferromagnetic, and ferrimagnetic. Table 8.2 provides a summary of the magnetic properties of these classes of materials.

8.2.1 DIAMAGNETISM

Typical diamagnetic materials have a magnetic susceptibility that is negative and small. For example, the silicon crystal is diamagnetic with $\chi_m = -5.2 \times 10^{-6}$. The relative permeability of diamagnetic materials is slightly less than unity. When a diamagnetic substance such as a silicon crystal is placed in a magnetic field, the magnetization vector **M** in the material is in the *opposite* direction to the applied field $\mu_o\mathbf{H}$ and the resulting field **B** within the material is less than $\mu_o\mathbf{H}$. The negative susceptibility can be interpreted as the diamagnetic substance trying to expel the applied field from the material. When a diamagnetic specimen is placed in a nonuniform magnetic field, the magnetization **M** of the material is in the opposite direction to **B** and the specimen experiences a net force toward smaller fields, as depicted in Figure 8.12. A substance exhibits diamagnetism whenever the constituent atoms in the material have closed subshells and shells. This means that each constituent atom has no permanent magnetic moment in the absence of an applied field. Covalent

Table 8.2 Classification of magnetic materials

Type	χ_m (typical values)	χ_m versus T	Comments and Examples
Diamagnetic	Negative and small (-10^{-6})	T independent	Atoms of the material have closed shells. Organic materials, *e.g.*, many polymers; covalent solids, *e.g.*, Si, Ge, diamond; some ionic solids, *e.g.*, alkalihalides; some metals, *e.g.*, Cu, Ag, Au.
	Negative and large (-1)	Below a critical temperature	Superconductors
Paramagnetic	Positive and small (10^{-5}–10^{-4})	Independent of T	Due to the alignment of spins of conduction electrons. Alkali and transition metals.
	Positive and small (10^{-5})	Curie or Curie–Weiss law, $\chi_m = C/(T - T_C)$	Materials in which the constituent atoms have a permanent magnetic moment, *e.g.*, gaseous and liquid oxygen; ferromagnets (Fe), antiferromagnets (Cr), and ferrimagnets (Fe_3O_4) at high temperatures.
Ferromagnetic	Positive and very large	Ferromagnetic below and paramagnetic above the Curie temperature	May possess a large permanent magnetization even in the absence of an applied field. Some transition and rare earth metals, Fe, Co, Ni, Gd, Dy.
Antiferromagnetic	Positive and small	Antiferromagnetic below and paramagnetic above the Néel temperature	Mainly salts and oxides of transition metals, *e.g.*, MnO, NiO, MnF_2, and some transition metals, α–Cr, Mn.
Ferrimagnetic	Positive and very large	Ferrimagnetic below and paramagnetic above the Curie temperature	May possess a large permanent magnetization even in the absence of an applied field. Ferrites.

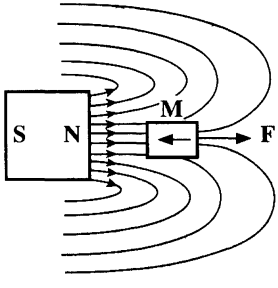

Figure 8.12 A diamagnetic material placed in a nonuniform magnetic field experiences a force toward smaller fields. This repels the diamagnetic material away from a permanent magnet.

crystals and many ionic crystals are typical diamagnetic materials because the constituent atoms have no unfilled subshells. Superconductors, as we will discuss later, are perfect diamagnets with $\chi_m = -1$ and totally expel the applied field from the material.

8.2.2 PARAMAGNETISM

Paramagnetic materials have a small positive magnetic susceptibility. For example, oxygen gas is paramagnetic with $\chi_m = 2.1 \times 10^{-6}$ at atmospheric pressure and room temperature. Each oxygen molecule has a net magnetic dipole moment $\boldsymbol{\mu}_{\text{mol}}$. In the absence of an applied field, these molecular moments are randomly oriented due to the random collisions of the molecules, as depicted in Figure 8.13a. The magnetization of the gas is zero. In the presence of an applied field, the molecular magnetic moments take various alignments with the field, as illustrated in Figure 8.13b. The degree of alignment of $\boldsymbol{\mu}_{\text{mol}}$ with the applied field and hence magnetization **M** increases with the strength of the applied field $\mu_o\mathbf{H}$. Magnetization M typically decreases with increasing temperature because at higher temperatures there are more molecular collisions, which destroy the alignments of molecular magnetic moments with the applied field. When a paramagnetic substance is placed in a nonuniform magnetic field, the induced magnetization **M** is along **B** and there is a net force toward greater fields. For example, when liquid oxygen is poured close to a strong magnet, as depicted in Figure 8.14, the liquid becomes attracted to the magnet.

Many metals are also paramagnetic, such as magnesium with $\chi_m = 1.2 \times 10^{-5}$. The origin of paramagnetism (called **Pauli spin paramagnetism**) in these metals is due to the alignment of the majority of spins of conduction electrons with the field.

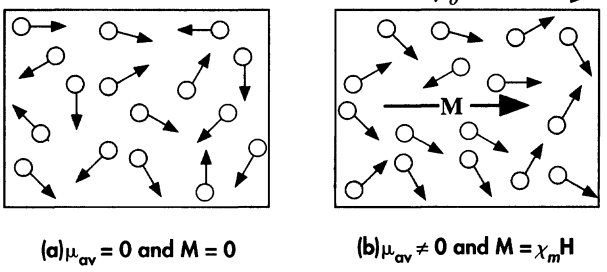

Figure 8.13
(a) In a paramagnetic material, each individual atom possesses a permanent magnetic moment, but due to thermal agitation there is no average moment per atom and $\mathbf{M} = 0$.
(b) In the presence of an applied field, individual magnetic moments take alignments along the applied field and **M** is finite and along **B**.

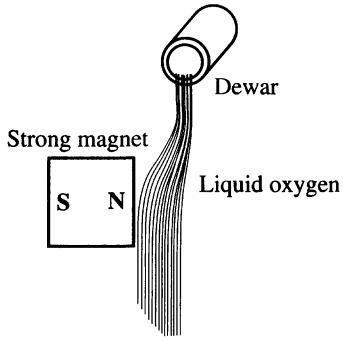

Figure 8.14 A paramagnetic material placed in a nonuniform magnetic field experiences a force toward greater fields.
This attracts the paramagnetic material (*e.g.*, liquid oxygen) toward a permanent magnet.

8.2.3 FERROMAGNETISM

Ferromagnetic materials such as iron can possess large permanent magnetizations even in the absence of an applied magnetic field. The magnetic susceptibility χ_m is typically positive and very large (even infinite) and, further, depends on the applied field intensity. The relationship between the magnetization **M** and the applied magnetic field $\mu_o\mathbf{H}$ is highly nonlinear. At sufficiently high fields, the magnetization **M** of the ferromagnet saturates. The origin of ferromagnetism is the quantum mechanical exchange interaction (discussed later) between the constituent atoms that results in regions of the material possessing permanent magnetization. Figure 8.15 depicts a region of the Fe crystal, called a **magnetic domain,** that has a net magnetization vector **M** due to the alignment of the magnetic moments of all Fe atoms in this region. This crystal domain has **magnetic ordering** as all the atomic magnetic moments have been aligned parallel to each other. Ferromagnetism occurs below a critical temperature called the Curie temperature T_C. At temperatures above T_C, ferromagnetism is lost and the material becomes paramagnetic.

8.2.4 ANTIFERROMAGNETISM

Antiferromagnetic materials such as chromium have a small but positive susceptibility. They cannot possess any magnetization in the absence of an applied field, in contrast to ferromagnets. Antiferromagnetic materials possess a magnetic ordering in which the magnetic moments of alternating atoms in the crystals align in opposite directions, as schematically depicted in Figure 8.16. The opposite alignments of atomic magnetic moments are due to quantum mechanical exchange forces (described later in Section 8.3). The net result is that in the absence of an applied field, there is no net magnetization. Antiferromagnetism occurs below a critical temperature called the **Néel temperature** T_N. Above T_N, antiferromagnetic material becomes paramagnetic.

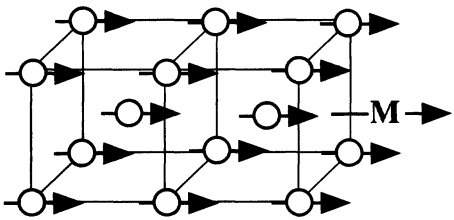

Figure 8.15 In a magnetized region of a ferromagnetic material such as iron, all the magnetic moments are spontaneously aligned in the same direction.

There is a strong magnetization vector **M** even in the absence of an applied field.

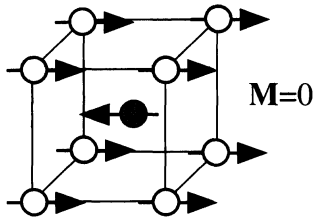

Figure 8.16 In this antiferromagnetic BCC crystal (Cr), the magnetic moment of the center atom is canceled by the magnetic moments of the corner atoms (one-eighth of the corner atom belongs to the unit cell).

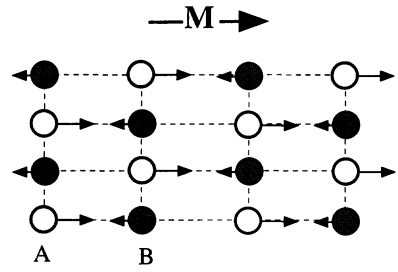

Figure 8.17 Illustration of magnetic ordering in the ferrimagnetic crystal.
All A atoms have their spins aligned in one direction and all B atoms have their spins aligned in the opposite direction. As the magnetic moment of an A atom is greater than that of a B atom, there is net magnetization **M** in the crystal.

8.2.5 FERRIMAGNETISM

Ferrimagnetic materials such as ferrites (*e.g.*, Fe_3O_4) exhibit magnetic behavior similar to ferromagnetism below a critical temperature called the Curie temperature T_C. Above T_C they become paramagnetic. The origin of ferrimagnetism is based on magnetic ordering, as schematically illustrated in Figure 8.17. All A atoms have their spins aligned in one direction and all B atoms have their spins aligned in the opposite direction. As the magnetic moment of an A atom is greater than that of a B atom, there is net magnetization **M** in the crystal. Unlike the antiferromagnetic case, the oppositely directed magnetic moments have different magnitudes and do not cancel. The net effect is that the crystal can possess magnetization even in the absence of an applied field. Since ferrimagnetic materials are typically nonconducting and therefore do not suffer from eddy current losses, they are widely used in high-frequency electronics applications.

All useful magnetic materials in electrical engineering are invariably ferromagnetic or ferrimagnetic.

8.3 FERROMAGNETISM ORIGIN AND THE EXCHANGE INTERACTION

The transition metals iron, cobalt, and nickel are all ferromagnetic at room temperature. The rare earth metals gadolinium and dysprosium are ferromagnetic below room temperature. Ferromagnetic materials can exhibit permanent magnetization even in the absence of an applied field; that is, they possess a susceptibility that is infinite.

In a magnetized iron crystal, all the atomic magnetic moments are aligned in the same direction, as illustrated in Figure 8.15, where the moments in this case have all been aligned along the [100] direction, which gives net magnetization along this direction. It may be thought that the reason for the alignment of the moments is the magnetic forces between the moments, just as bar magnets will tend to align head to tail in an SNSN . . . fashion. This is not, however, the cause, as the magnetic potential energy of interaction is small, indeed smaller than the thermal energy.

The iron atom has the electron structure $[Ar]3d^64s^2$. An isolated iron atom has only the $3d$ subshell with four of the five orbitals unfilled. By virtue of Hund's rule, the electrons try to align their spins so that the five $3d$ orbitals contain two paired electrons

Figure 8.18 The isolated Fe atom has four unpaired spins and a spin magnetic moment of 4β.

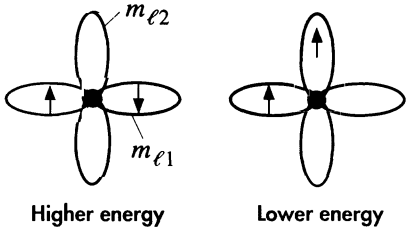

Figure 8.19 Hund's rule for an atom with many electrons is based on the exchange interaction.

and four unpaired electrons, as in Figure 8.18. The isolated atom has four parallel electron spins and hence a spin magnetic moment of 4β.

The origin of Hund's rule, visualized in Figure 8.19, lies in the fact that when the spins are parallel (same m_s), as a requirement of the Pauli exclusion principle, the electrons must occupy orbitals with different m_ℓ and hence possess different spatial distributions (recall that m_ℓ determines the orientation of an orbit). Different m_ℓ values result in a smaller Coulombic repulsion energy between the electrons compared with the case where the electrons have opposite spins (different m_s), where they would be in the same orbital (same m_ℓ), that is, in the same spatial region. It is apparent that even though the interaction energy between the electrons has nothing to do with magnetic forces, it does depend nonetheless on the orientations of their spins (m_s), or on their spin magnetic moments, and it is less when the spins are parallel. Two electrons parallel their spins not because of the direct magnetic interaction between the spin magnetic moments but because of the **Pauli exclusion principle** and the **electrostatic interaction energy.** Together they constitute what is known as an **exchange interaction,** which forces two electrons to take m_s and m_ℓ values that result in the minimum of electrostatic energy. In an atom, the exchange interaction therefore forces two electrons to take the same m_s but different m_ℓ if this can be done within the Pauli exclusion principle. This is the reason an isolated Fe atom has four unpaired spins in the $3d$ subshell.

In the crystal, of course, the outer electrons are no longer strictly confined to their parent Fe atoms, particularly the $4s$ electrons. The electrons now have wavefunctions that belong to the whole solid. Something like Hund's rule also operates at the crystal level for Fe, Co, and Ni. If two $3d$ electrons parallel their spins and occupy different wavefunctions (and hence different negative charge distributions), the resulting mutual Coulombic repulsion between them and also with all the other electrons and the attraction to the positive Fe ions result in an overall reduction of potential energy. This reduction in energy is again due to the exchange interaction and is a direct consequence of the Pauli exclusion principle and the Coulombic forces. Thus, the majority of $3d$ electrons spontaneously parallel their spins without the need for the application of an external magnetic field. The number of electrons that actually parallel their spins depends on the strength of the exchange interaction, and for the iron crystal this turns out to be about 2.2 electrons per atom. Since typically the wavefunctions

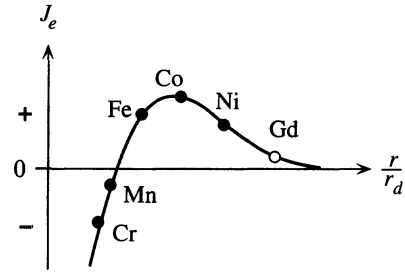

Figure 8.20 The exchange integral as a function of r/r_d, where r is the interatomic distance and r_d the radius of the d orbit (or the average d subshell radius). Cr to Ni are transition metals. For Gd, the x axis is r/r_f, where r_f is the radius of the f orbit.

of the $3d$ electrons in the whole iron crystal show localization around the iron ions, some people prefer to view the $3d$ electrons as spending the majority of their time around Fe atoms, which explains the reason for drawing the magnetized iron crystal as in Figure 8.15.

It may be thought that all solids should follow the example of Fe and become spontaneously ferromagnetic since paralleling spins would result in different spatial distributions of negative charge and probably a reduction in the electrostatic energy, but this is not generally the case at all. We know that, in the case of covalent bonding, the electrons have the lowest energy when the two electrons spin in opposite directions. In covalent bonding in molecules, the exchange interaction does not reduce the energy. Making the electron spins parallel leads to spatial negative charge distributions that result in a net mutual electrostatic repulsion between the positive nuclei.

In the simplest case, for two atoms only, the exchange energy depends on the interatomic separation between two interacting atoms and the relative spins of the two outer electrons (labeled as 1 and 2). From quantum mechanics, the exchange interaction can be represented in terms of an exchange energy E_{ex} as

$$E_{ex} = -2J_e \mathbf{S}_1 \cdot \mathbf{S}_2 \qquad [8.21]$$

where $\mathbf{S}_1$ and $\mathbf{S}_2$ are the spin angular momenta of the two electrons and J_e is a numerical quantity called the **exchange integral** that involves integrating the wavefunctions with the various potential energy interaction terms. It therefore depends on the electrostatic interactions and hence on the interatomic distance. For the majority of solids, J_e is negative, so the exchange energy is negative if $\mathbf{S}_1$ and $\mathbf{S}_2$ are in the opposite directions, that is, the spins are antiparallel (as we found in covalent bonding). This is the antiferromagnetic state. For Fe, Co, and Ni, however, J_e is positive. E_{ex} is then negative if $\mathbf{S}_1$ and $\mathbf{S}_2$ are parallel. Spins of the $3d$ electrons on the Fe atoms therefore spontaneously align in the same direction to reduce the exchange energy. This spontaneous magnetization is the phenomenon of ferromagnetism. Figure 8.20 illustrates how J_e changes with the ratio of interatomic separation to the radius of the $3d$ subshell (r/r_d). For the transition metals Fe, Co, and Ni, the r/r_d is such that J_e is positive.[3] In all other cases, it is negative and does not produce ferromagnetic behavior. It should be

[3] According to H. P. Myers, *Introductory Solid State Physics* 2nd ed., London: Taylor and Francis Ltd., 1997, p. 362, there have been no theoretical calculations of the exchange integral J_e for any real magnetic substance.

mentioned that Mn, which is not ferromagnetic, can be alloyed with other elements to increase r/r_d and hence endow ferromagnetism in the alloy.

EXAMPLE 8.3

SATURATION MAGNETIZATION IN IRON The maximum magnetization, called **saturation magnetization** M_{sat}, in iron is about 1.75×10^6 A m^{-1}. This corresponds to all possible net spins aligning parallel to each other. Calculate the effective number of Bohr magnetons per atom that would give M_{sat}, given that the density and relative atomic mass of iron are 7.86 g cm^{-3} and 55.85, respectively.

SOLUTION

The number of Fe atoms per unit volume is

$$n_{at} = \frac{\rho N_A}{M_{at}} = \frac{(7.86 \times 10^3 \text{ kg m}^{-3})(6.022 \times 10^{23} \text{ mol}^{-1})}{55.85 \times 10^{-3} \text{ kg mol}^{-1}}$$

$$= 8.48 \times 10^{28} \text{ atoms m}^{-3}$$

If each Fe atom contributes x number of net spins, then since each net spin has a magnetic moment of β, we have,

$$M_{sat} = n_{at}(x\beta)$$

so

$$x = \frac{M_{sat}}{n_{at}\beta} = \frac{1.75 \times 10^6}{(8.48 \times 10^{28})(9.27 \times 10^{-24})} \approx 2.2$$

In the solid, each Fe atom contributes only 2.2 Bohr magnetons to the magnetization even though the isolated Fe atom has 4 Bohr magnetons. There is no orbital contribution to the magnetic moment per atom in the solid because all the outer electrons, $3d$ and $4s$ electrons, can be viewed as belonging to the whole crystal, or being in an energy band, rather than orbiting individual atoms. A $3d$ electron is attracted by various Fe ions in the crystal and therefore does not experience a central force, in contrast to the $3d$ electron in the isolated Fe atom that orbits the nucleus. The orbital momentum in the crystal is said to be quenched.

We should note that when the magnetization is saturated, all atomic magnetic moments are aligned. The resulting magnetic field within the iron specimen in the absence of an applied magnetizing field ($H = 0$) is

$$B_{sat} = \mu_o M_{sat} = 2.2 \text{ T}$$

8.4 SATURATION MAGNETIZATION AND CURIE TEMPERATURE

The maximum magnetization in a ferromagnet when all the atomic magnetic moments have been aligned as much as possible is called the saturation magnetization M_{sat}. In the iron crystal, for example, this corresponds to each Fe atom with an effective spin magnetic moment of 2.2 Bohr magnetons aligning in the same direction to give a magnetic field $\mu_o M_{sat}$ or 2.2 T. As we increase the temperature, lattice vibrations become more energetic, which leads to a frequent disruption of the alignments of the spins. The spins cannot align perfectly with each other as the temperature increases due to lattice vibrations

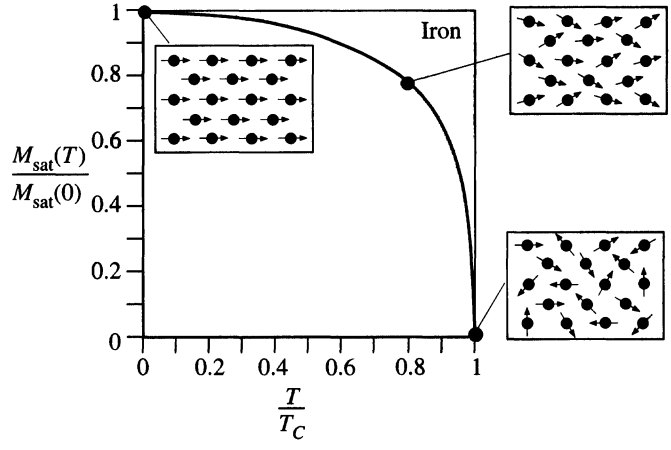

Figure 8.21 Normalized saturated magnetization versus reduced temperature T/T_C where T_C is the Curie temperature (1043 K).

randomly agitating the individual spins. When an energetic lattice vibration passes through a spin site, the energy in the vibration may be sufficient to disorientate the spin of the atom. The ferromagnetic behavior disappears at a critical temperature called the **Curie temperature,** denoted by T_C, when the thermal energy of lattice vibrations in the crystal can overcome the potential energy of the exchange interaction and hence destroy the spin alignments. Above the Curie temperature, the crystal behaves as if it were paramagnetic. The saturation magnetization M_{sat}, therefore, decreases from its maximum value $M_{sat}(0)$ at absolute zero of temperature to zero at the Curie temperature. Figure 8.21 shows the dependence of M_{sat} on the temperature when M_{sat} has been normalized to $M_{sat}(0)$ and the temperature is the reduced temperature, that is, T/T_C. At $T/T_C = 1$, $M_{sat} = 0$. When plotted in this way, the ferromagnets cobalt and nickel follow closely the observed behavior for iron. We should note that since for iron $T_C = 1043$ K, at room temperature, $T/T_C = 0.29$ and M_{sat} is very close to its value at $M_{sat}(0)$.

Since at the Curie temperature, the thermal energy, of the order of kT_C, is sufficient to overcome the energy of the exchange interaction E_{ex} that aligns the spins, we can take kT_C as an order of magnitude estimate of E_{ex}. For iron, E_{ex} is ~0.09 eV and for cobalt this is ~0.1 eV.

Table 8.3 summarizes some of the important properties of the ferromagnets Fe, Co, Ni, and Gd (rare earth metal).

Table 8.3 Properties of the ferromagnets Fe, Co, Ni, and Gd

	Fe	Co	Ni	Gd
Crystal structure	BCC	HCP	FCC	HCP
Bohr magnetons per atom	2.22	1.72	0.60	7.1
$M_{sat}(0)$ (MA m^{-1})	1.75	1.45	0.50	2.0
$B_{sat} = \mu_o M_{sat}$(T)	2.2	1.82	0.64	2.5
T_C	770 °C	1127 °C	358 °C	16 °C
	1043 K	1400 K	631 K	289 K

8.5 MAGNETIC DOMAINS: FERROMAGNETIC MATERIALS

8.5.1 MAGNETIC DOMAINS

A single crystal of iron does not necessarily possess a net permanent magnetization in the absence of an applied field. If a magnetized piece of iron is heated to a temperature above its Curie temperature and then allowed to cool in the absence of a magnetic field, it will possess no net magnetization. The reason for the absence of net magnetization is due to the formation of magnetic domains that effectively cancel each other, as discussed below. A **magnetic domain** is a region of the crystal in which all the spin magnetic moments are aligned to produce a magnetic moment in one direction only.

Figure 8.22a shows a single crystal of iron that has a permanent magnetization as a result of ferromagnetism (aligning of all atomic spins). The crystal is like a bar magnet with magnetic field lines around it. As we know, there is potential energy (*PE*), called **magnetostatic energy,** stored in a magnetic field, and we can reduce this energy in the external field by dividing the crystal into two domains where the magnetizations are in the opposite directions, as shown in Figure 8.22b. The external magnetic field lines are reduced and there is now less potential energy stored in the magnetic field. There are only field lines at the ends. This arrangement is energetically favorable because the magnetostatic energy has been reduced by decreasing the external field

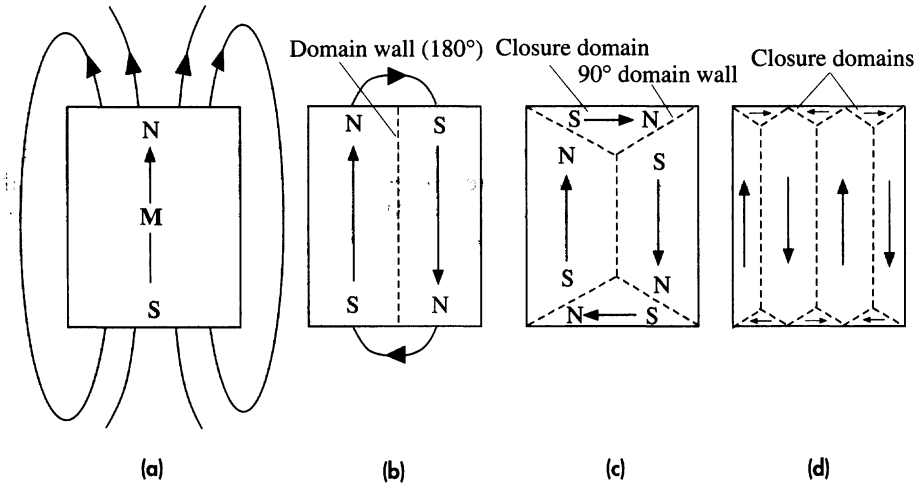

Figure 8.22

(a) Magnetized bar of ferromagnet in which there is only one domain and hence an external magnetic field.

(b) Formation of two domains with opposite magnetizations reduces the external field. There are, however, field lines at the ends.

(c) Domains of closure fitting at the ends eliminate the external fields at the ends.

(d) A specimen with several domains and closure domains. There is no external magnetic field and the specimen appears unmagnetized.

lines. However, there is now a boundary, called a **domain wall** (or **Bloch wall**), between the two domains where the magnetization changes from one direction to the opposite direction and hence the atomic spins do, also. It requires energy to rotate the atomic spin through 180° with respect to its neighbor because the exchange energy favors aligning neighboring atomic spins (0°). The wall in Figure 8.22b is a 180° wall inasmuch as the magnetization through the wall is rotated by 180°. It is apparent that the wall region where the neighboring atomic spins change their relative direction (or orientation) from one domain to the neighboring one has higher *PE* than the bulk of the domain, where all the atomic spins are aligned. As we will show below, the domain wall is not simply one atomic spacing but has a finite thickness, which for iron is typically of the order of 0.1 μm, or several hundred atomic spacings. The excess energy in the wall increases with the area of the wall.

The magnetostatic energy associated with the field lines at the ends in Figure 8.22b can be further reduced by eliminating these external field lines by closing the ends with sideway domains with magnetizations at 90°, as shown in Figure 8.22c. These end domains are **closure domains** and have walls that are 90° walls. The magnetization is rotated through 90° through the wall. Although we have reduced the magnetostatic energy, we have increased the potential energy in the walls by adding additional walls. The creation of magnetic domains continues (spontaneously) until the potential energy reduction in creating an additional domain is the same as the increase in creating an additional wall. The specimen then possesses minimum potential energy and is in equilibrium with no net magnetization. Figure 8.22d shows a specimen with several domains and no net magnetization. The sizes, shapes, and distributions of domains depend on a number of factors, including the size and shape of the whole specimen. For iron particles of dimensions less than of the order of 0.01 μm, the increase in the potential energy in creating a domain wall is too costly and these particles are single domains and hence always magnetized.

The magnetization of each domain is normally along one of the preferred directions in which the atomic spin alignments are easiest (the exchange interaction is the strongest). For iron, the magnetization is easiest along any one of six ⟨100⟩ directions (along cube edges), which are called **easy directions.** The domains have magnetizations along these easy directions. The magnetization of the crystal along an applied field occurs, in principle, by the growth of domains with magnetizations (or components of **M**) along the applied field (**H**), as illustrated in Figure 8.23a and b. For simplicity, the magnetizing field is taken along an easy direction. The Bloch wall between the domains A and B migrates toward the right, which enlarges the domain A and shrinks domain B, with the net result that the crystal has an effective magnetization **M** along **H**. The migration of the Bloch wall is caused by the spins in the wall, and also spins in section B adjacent to the wall, being gradually rotated by the applied field (they experience a torque). The magnetization process therefore involves the motions of Bloch walls in the crystal.

8.5.2 MAGNETOCRYSTALLINE ANISOTROPY

Ferromagnetic crystals characteristically exhibit magnetic anisotropy, which means that the magnetic properties are different along different crystal directions. In the case of iron (BCC), the spins in a domain are most easily aligned in any of the six [100] type

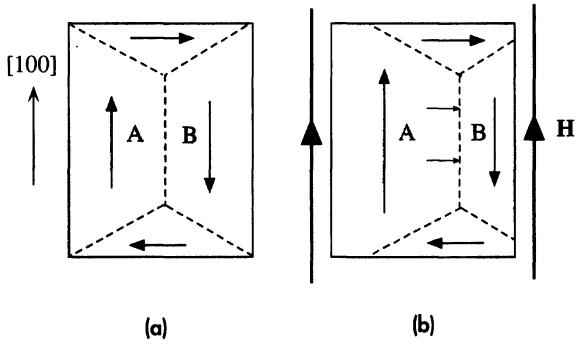

Figure 8.23
(a) An unmagnetized crystal of iron in the absence of an applied magnetic field. Domains A and B are the same size and have opposite magnetizations.
(b) When an external magnetic field is applied, the domain wall migrates into domain B, which enlarges A and shrinks B. The result is that the specimen now acquires net magnetization.

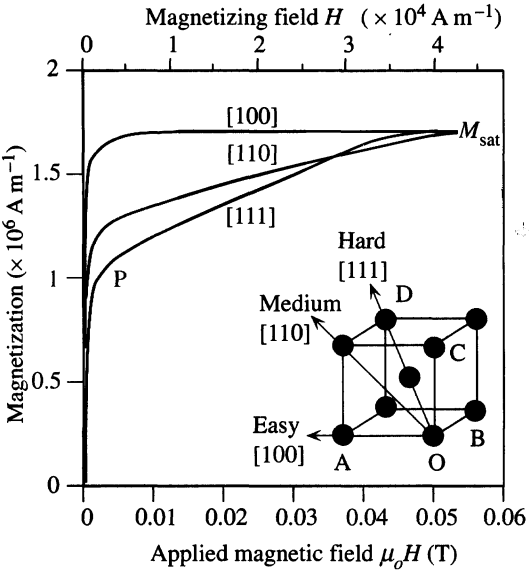

Figure 8.24 Magnetocrystalline anisotropy in a single iron crystal.
M versus H depends on the crystal direction and is easiest along [100] and hardest along [111].

directions, collectively labeled as ⟨100⟩, and correspond to the six edges of the cubic unit cell. The exchange interactions are such that spin magnetic moments are most easily aligned with each other if they all point in one of the six ⟨100⟩ directions. Thus ⟨100⟩ directions in the iron crystal constitute the easy directions for magnetization. When a magnetizing field **H** along a [100] direction is applied, as illustrated in Figure 8.23a and b, domain walls migrate to allow those domains (*e.g.*, A) with magnetizations along **H** to grow at the expense of those domains (*e.g.*, B) with magnetizations opposing **H**. The observed M versus H behavior is shown in Figure 8.24. Magnetization rapidly increases and saturates with an applied field of less than 0.01 T.

On the other hand, if we want to magnetize the crystal along the [111] direction by applying a field along this direction, then we have to apply a stronger field than that along [100]. This is clearly shown in Figure 8.24, where the resulting magnetization along [111] is smaller than that along [100] for the same magnitude of applied field. Indeed, saturation is reached at an applied field that is about a factor of 4 greater than

Table 8.4 Exchange interaction, magnetocrystalline anisotropy energy K, and saturation magnetostriction coefficient λ_{sat}

Material	Crystal	$E_{ex} \approx kT_C$ (meV)	Easy	Hard	K (mJ cm^{-3})	λ_{sat} ($\times 10^{-6}$)
Fe	BCC	90	<100>; cube edge	<111>; cube diagonal	48	20 [100] −20 [111]
Co	HCP	120	// to c axis	⊥ to c axis	450	
Ni	FCC	50	<111>; cube diagonal	<100>; cube edge	5	−46 [100] −24 [111]

NOTE: K is the magnitude of what is called the first anisotropy constant (K_1) and is approximately the magnitude of the anisotropy energy. E_{ex} is an estimate from kT_C, where T_C is the Curie temperature. All approximate values are from various sources. (Further data can be found in D. Jiles, *Introduction to Magnetism and Magnetic Materials*, London, England: Chapman and Hall, 1991.)

that along [100]. The [111] direction in the iron crystal is consequently known as the **hard direction.** The M versus H behavior along [100], [110], and [111] directions in an iron crystal and the associated anisotropy are shown in Figure 8.24.

When an external field is applied along the diagonal direction OD in Figure 8.24, initially all those domains with **M** along OA, OB, and OC, that is, those with magnetization components along OD, grow by consuming those with **M** in the wrong direction and eventually take over the whole specimen. This is an easy process (similar to the process along [100]) and requires small fields and represents the processes from 0 to P on the magnetization curve for [111] in Figure 8.24. However, from P onwards, the magnetizations in the domains have to be rotated away from their easy directions, that is, from OA, OB, and OC toward OD. This process consumes substantial energy and hence needs much stronger applied fields.

It is apparent that the magnetization of the crystal along [100] needs the least energy, whereas that along [111] consumes the greatest energy. The excess energy required to magnetize a unit volume of a crystal in a particular direction with respect to that in the easy direction is called the **magnetocrystalline anisotropy energy** and is denoted by K. For iron, the anisotropy energy is zero for [100] and largest for the [111] direction, about 48 kJ m^{-3} or 3.5×10^{-6} eV per atom. For cobalt, which has the HCP crystal structure, the anisotropy energy is at least an order of magnitude greater. Table 8.4 summarizes the easy and hard directions, and the anisotropy energy K for the hard direction.

8.5.3 DOMAIN WALLS

We recall that the spin magnetic moments rotate across a domain wall. We mentioned that the wall is not simply one atomic spacing wide, as this would mean two neighboring spins being at 180° to each other and hence possessing excessive exchange interaction. A schematic illustration of the structure of a typical 180° Bloch wall, between two domains A and B, is depicted in Figure 8.25. It can be seen that the neighboring spin magnetic moments are rotated gradually, and over several hundred atomic spacings the magnetic moment reaches a rotation of 180°. Exchange

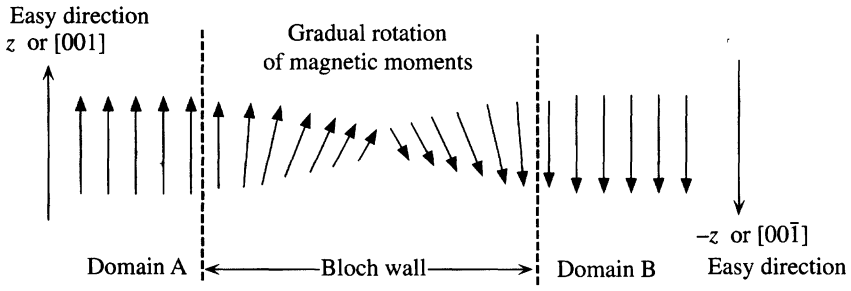

Figure 8.25 In a Bloch wall, the neighboring spin magnetic moments rotate gradually, and it takes several hundred atomic spacings to rotate the magnetic moment by 180°.

forces between neighboring atomic spins favor very little relative rotation. Had it been left to exchange forces alone, relative rotation of neighboring spins would be so minute that the wall would have to be very thick (infinitely thick) to achieve a 180° rotation.

However, magnetic moments that are oriented away from the easy direction possess excess energy, called the anisotropy energy (K). If the wall is thick, then it will contain many magnetic moments rotated away from the easy direction and there would be a substantial anisotropy energy in the wall. Minimum anisotropy energy in the wall is obtained when the magnetic moment changes direction by 180° from the easy direction along $+z$ to that along $-z$ in Figure 8.25 without any intermediate rotations away from z. This requires a wall of one atomic spacing. In reality, the wall thickness is a compromise between the exchange energy, demanding a thick wall, and anisotropy energy, demanding a thin wall. The equilibrium wall thickness is that which minimizes the total potential energy, which is the sum of the exchange energy *and* the anisotropy energy within the wall. This thickness turns out to be ~ 0.1 μm for iron and less for cobalt, in which the anisotropy energy is greater.

EXAMPLE 8.4

MAGNETIC DOMAIN WALL ENERGY AND THICKNESS The Bloch wall energy and thickness depend on two main factors: the exchange energy E_{ex} (J atom^{-1}) and magnetocrystalline energy K (J m^{-3}). Suppose that we consider a Bloch wall of unit area, and thickness δ, and calculate the potential energy U_{wall} in this wall due to the exchange energy and the magnetocrystalline anisotropy energy. The spins change by 180° across the thickness δ of the Bloch wall as in Figure 8.25. The contribution $U_{exchange}$ from the exchange energy arises because it takes energy to rotate one spin with respect to another. If the thickness δ is large, then the angular change from one spin to the next will be small, and the exchange energy contribution $U_{exchange}$ will also be small. Thus, $U_{exchange}$ is inversely proportional to δ. $U_{exchange}$ is also directly proportional to E_{ex} which gauges the magnitude of this exchange energy; it costs E_{ex} to rotate the two spins 180° to each other. Thus, $U_{exchange} \propto E_{ex}/\delta$.

The anisotropy energy contribution $U_{anisotropy}$ arises from having spins point away from the easy direction. If the thickness δ is large, there are more and more spin moments that are aligned away from the easy direction, and the anisotropy energy contribution $U_{anisotropy}$ is also large. Thus, $U_{anisotropy}$ is proportional to δ, and also, obviously, to the anisotropy energy K that gauges the magnitude of this energy. Thus, $U_{anisotropy} \propto K\delta$.

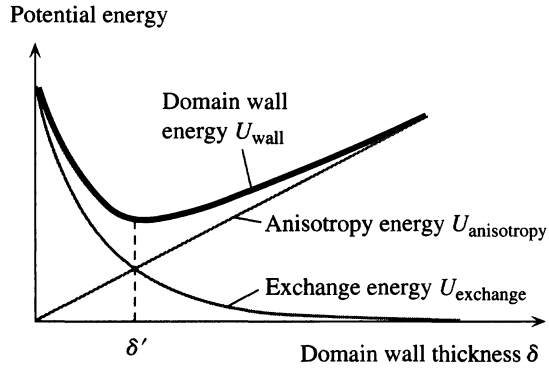

Figure 8.26 The potential energy of a domain wall depends on the exchange and anisotropy energies.

Figure 8.26 shows the contributions of the exchange and anisotropy energies, $U_{exchange}$ and $U_{anisotropy}$, to the total Bloch wall energy as a function of wall thickness δ. It is clear that exchange and anisotropy energies have opposite (or conflicting) requirements on the wall thickness. There is, however, an optimum thickness δ' that *minimizes* the Bloch wall energy, that is, a thickness that balances the requirements of exchange and anisotropy forces.

If the interatomic spacing is a, then there would be $N = \delta/a$ atomic layers in the wall. Since the spin moment angle changes by 180° across δ, we can calculate the relative spin orientations $(180°/N)$ of adjacent atomic layers, and hence we can find the exact contributions of exchange and anisotropy energies. We do not need the exact mathematics, but the final result is that the potential energy U_{wall} per unit area of the wall is approximately

Potential energy of a Bloch wall

$$U_{wall} \approx \frac{\pi^2 E_{ex}}{2a\delta} + K\delta$$

The first term on the right is the exchange energy contribution (proportional to E_{ex}/δ), and the second is the anisotropy energy contribution (proportional to $K\delta$); both have the features we discussed.

Show that the minimum energy occurs when the wall has the thickness

Bloch wall thickness

$$\delta' = \left(\frac{\pi^2 E_{ex}}{2aK}\right)^{1/2}$$

Taking $E_{ex} \approx kT_C$, where T_C is the Curie temperature, and for iron, $K \approx 50$ kJ m^{-3}, and $a \approx 0.3$ nm, estimate the thickness of a Bloch wall and its energy per unit area.

SOLUTION

We can differentiate U_{wall} with respect to δ,

$$\frac{dU_{wall}}{d\delta} = -\frac{\pi^2 E_{ex}}{2a\delta^2} + K$$

and then set it to zero for $\delta = \delta'$ to find,

$$\delta' = \left(\frac{\pi^2 E_{ex}}{2aK}\right)^{1/2}$$

Since $T_C = 1043$ K, $E_{ex} = kT_C = (1.38 \times 10^{-23}\ \text{J K}^{-1})(1043\ \text{K}) = 1.4 \times 10^{-20}$ J, so that

$$\delta' = \left(\frac{\pi^2 E_{ex}}{2aK}\right)^{1/2} = \left[\frac{\pi^2(1.4 \times 10^{-20})}{2(0.3 \times 10^{-9})(50,000)}\right]^{1/2} = 6.8 \times 10^{-8}\text{m} \quad \text{or} \quad 68\ \text{nm}$$

and $$U_{\text{wall}} = \frac{\pi^2 E_{\text{ex}}}{2a\delta'} + K\delta' = \frac{\pi^2(1.4 \times 10^{-20})}{2(0.3 \times 10^{-9})(6.8 \times 10^{-8})} + (50 \times 10^3)(6.8 \times 10^{-8})$$

$$= 0.007 \text{ J m}^{-2} \quad \text{or} \quad 7 \text{ mJ m}^{-2}$$

A better calculation gives δ' and U_{wall} as 40 nm and 3 mJ m^{-2}, respectively, about the same order of magnitude.[4] The Bloch wall thickness is roughly 70 nm or $\delta/a = 230$ atomic layers. It is left as an exercise to show that when $\delta = \delta'$, the exchange and anisotropy energy contributions are equal.

8.5.4 MAGNETOSTRICTION

If we were to strain a ferromagnetic crystal (by applying a suitable stress) along a certain direction, we would change the interatomic spacing not only along this direction but also in other directions and hence change the exchange interactions between the atomic spins. This would lead to a change in the magnetization properties of the crystal. In the converse effect, the magnetization of the crystal generates strains or changes in the physical dimensions of the crystal. For example, in very qualitative terms, when an iron crystal is magnetized along the [111] direction by a strong field, the atomic spins within domains are rotated from their easy directions toward the hard [111] direction. These electron spin rotations involve changes in the electron charge distributions around the atoms and therefore affect the interatomic bonding and hence the interatomic spacing. When an iron crystal is placed in a magnetic field along an easy direction [100], it gets longer along this direction but contracts in the transverse directions [010] and [001], as depicted in Figure 8.27. The reverse is true for nickel. The longitudinal strain $\Delta\ell/\ell$ along the direction of magnetization is called the **magnetostrictive constant,** denoted by λ. The magnetostrictive constant depends on the crystal direction and may be positive (extension) or negative (contraction). Further, λ depends on the applied field and can even change sign as the field is increased; for example, λ for iron along the [110] direction is initially positive and then, at higher fields, becomes negative. When the crystal reaches saturation magnetization, λ also reaches saturation, called **saturation magnetostriction strain** λ_{sat}, which is typically 10^{-6}–10^{-5}. Table 8.4 summarizes the λ_{sat} values for Fe and Ni along the easy and hard directions. The crystal lattice strain energy associated with magnetostriction is called the **magnetostrictive energy,** which is typically less than the anisotropy energy.

Magnetostriction is responsible for the transformer hum noise one hears near power transformers. As the core of a transformer is magnetized one way and then in the opposite direction under an alternating voltage, the alternating changes in the longitudinal strain vibrate the surrounding environment, air, oil, and so forth, and generate an acoustic noise at twice the main frequency, or 120 Hz, and its harmonics. (Why?)

The magnetostrictive constant can be controlled by alloying metals. For example, λ_{sat} along the easy direction for nickel is negative and for iron it is positive, but for the alloy 85% Ni–15% Fe, it is zero. In certain magnetic materials, λ can be quite large,

[4] See, for example, D. Jiles, *Introduction to Magnetism and Magnetic Materials*, London, England: Chapman and Hall, 1991.

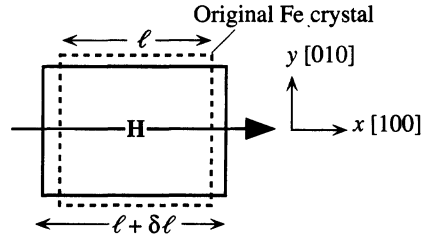

Figure 8.27 Magnetostriction means that the iron crystal in a magnetic field along *x*, an easy direction, elongates along *x* but contracts in the transverse directions (in low fields).

greater than 10^{-4}, which has opened up new areas of sensor applications based on the magnetostriction effect. For example, it may be possible to develop torque sensors for automotive steering applications by using Co-ferrite type magnetic materials[5] (*e.g.*, $CoO–Fe_2O_3$ or similar compounds) that have λ_{sat} of the order of 10^{-4}.

8.5.5 DOMAIN WALL MOTION

The magnetization of a single ferromagnetic crystal involves the motions of domain boundaries to allow the favorably oriented domains to grow at the expense of domains with magnetizations directed away from the field (Figure 8.23). The motion of a domain wall in a crystal is affected by crystal imperfections and impurities and is not smooth. For example, in a 90° Bloch wall, the magnetization changes direction by 90° across the boundary. Due to magnetostriction (Figure 8.27), there is a change in the distortion of the lattice across the 90° boundary, which leads to a complicated strain and hence stress distribution around this boundary. We also know that crystal imperfections such as dislocations and point defects also have strain and stress distributions around them. Domain walls and crystal imperfections therefore interact with each other. Dislocations are line defects that have a substantial volume of strained lattice around them. Figure 8.28 visualizes a dislocation with tensile and compressive strains around it and a domain wall that has a tensile strain on the side of the dislocation. If the wall gets close to the dislocation, the tensile and compressive strains cancel, which results in an unstrained lattice and hence a lower strain energy. This energetically favorable arrangement keeps the domain boundary close to the dislocation. It now takes greater magnetic field to snap away the boundary from the dislocation. Domain walls also interact with nonmagnetic impurities and inclusions. For example, an inclusion that finds itself in a domain becomes magnetized and develops south and north poles, as shown in Figure 8.29a. If the domain wall were to intersect the inclusion and if there were to be two neighboring domains around the inclusion, as in Figure 8.29b, then the magnetostatic energy would be lowered—energetically a favorable event. This reduction in magnetostatic potential energy means that it now takes greater force to move the domain wall past the impurity, as if the wall were "pinned" by the impurity.

The motion of a domain wall in a crystal is therefore not smooth but rather jerky. The wall becomes pinned somewhere by a defect or an impurity and then needs a

[5] See, for example, D. Jiles and C. C. H. Lo, *Sensors and Actuators*, **A106**, 3, 2003.

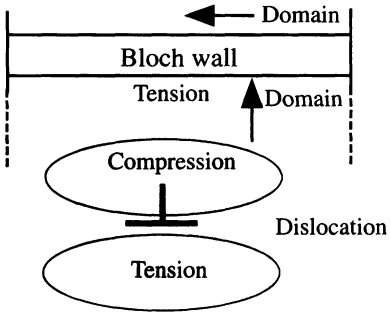

Figure 8.28 Stress and strain distributions around a dislocation and near a domain wall.

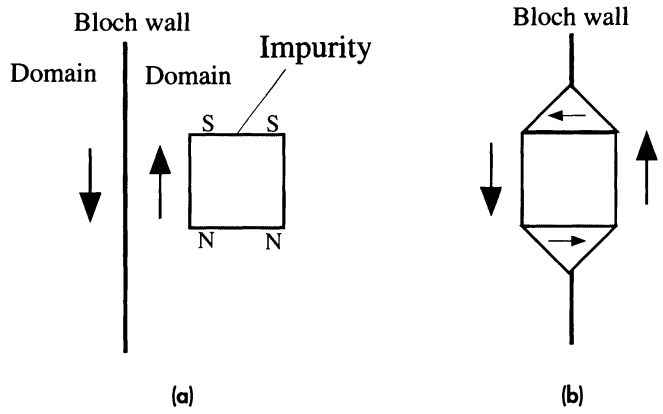

Figure 8.29 Interaction of a Bloch wall with a nonmagnetic (no permanent magnetization) inclusion.
(a) The inclusion becomes magnetized and there is magnetostatic energy.
(b) This arrangement has lower potential energy and is thus favorable.

greater applied field to break free. Once it snaps off, the domain wall is moved until it is attracted by another type of imperfection, where it is held until the field increases further to snap it away again. Each time the domain wall is snapped loose, lattice vibrations are generated, which means loss of energy as heat. The whole domain wall motion is nonreversible and involves energy losses as heat to the crystal.

8.5.6 POLYCRYSTALLINE MATERIALS AND THE M VERSUS H BEHAVIOR

The majority of the magnetic materials used in engineering are polycrystalline and therefore have a microstructure that consists of many grains of various sizes and orientations depending on the preparation and thermal history of the component. In an unmagnetized polycrystalline sample, each crystal grain will possess domains, as depicted in Figure 8.30. The domain structure in each grain will depend on the size and shape of the grain and, to some extent, on the magnetizations in neighboring grains. Although very small grains, perhaps smaller than 0.1 μm, may be single domains, in most cases the majority of the grains will have many domains. Overall, the structure will possess no net magnetization, provided that it was not previously subjected to an applied magnetic field. We can assume that the component was heated to a temperature above the Curie point and then allowed to cool to room temperature without an applied field.

Suppose that we start applying a very small external magnetic field ($\mu_o H$) along some direction, which we can arbitrarily label as $+x$. The domain walls within various grains begin to move small distances, and favorably oriented domains (those with a component of M along $+x$) grow a little larger at the expense of those pointing away from the field, as indicated by point a in Figure 8.31. The domain walls that are pinned by imperfections tend to bow out. There is a very small but net magnetization

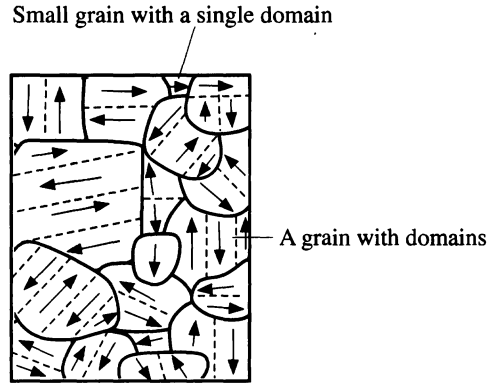

Figure 8.30 Schematic illustration of magnetic domains in the grains of an unmagnetized polycrystalline iron sample.
Very small grains have single domains.

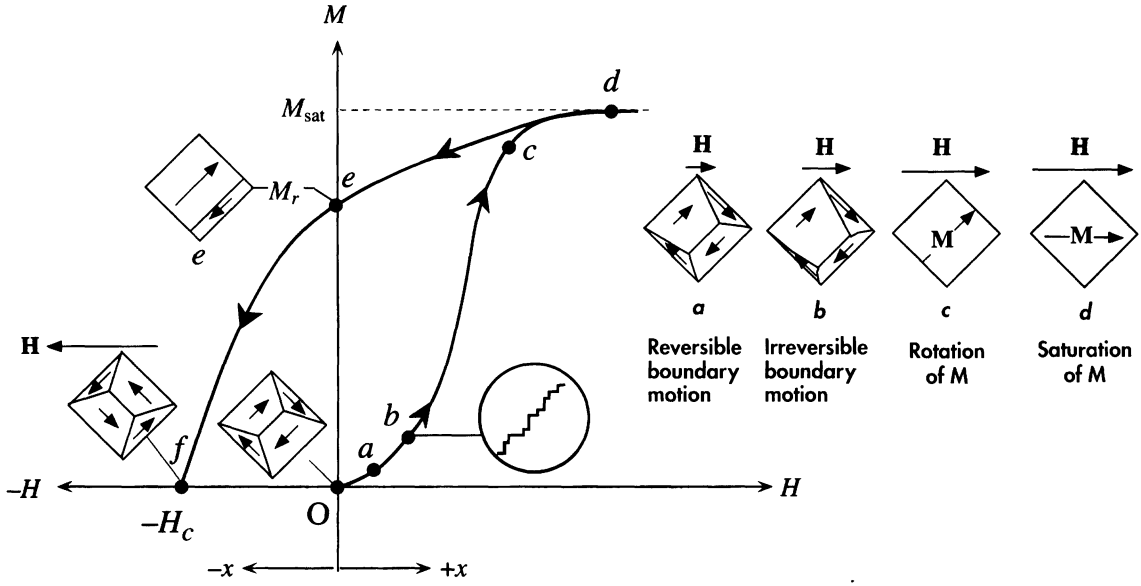

Figure 8.31 *M* versus *H* behavior of a previously unmagnetized polycrystalline iron specimen.
An example grain in the unmagnetized specimen is that at O.
(a) Under very small fields, the domain boundary motion is reversible.
(b) The boundary motions are irreversible and occur in sudden jerks.
(c) Nearly all the grains are single domains with saturation magnetizations in the easy directions.
(d) Magnetizations in individual grains have to be rotated to align with the field *H*.
(e) When the field is removed, the specimen returns along *d* to *e*.
(f) To demagnetize the specimen, we have to apply a magnetizing field of H_c in the reverse direction.

along the field, as indicated by the O*a* region in the magnetization versus magnetizing field (*M* versus *H*) behavior in Figure 8.31. As we increase the magnetizing field, the domain motions extend larger distances, as shown for point *b* in Figure 8.31, and walls encounter various obstacles such as crystal imperfections, impurities, second phases, and so on, which tend to attract the walls and thereby hinder their motions. A

domain wall that is stuck (or pinned) at an imperfection at a given field cannot move until the field increases sufficiently to provide the necessary force to snap the wall free, which then suddenly surges forward to the next obstacle. As a wall suddenly snaps free and shoots forward to the next obstacle, essentially two causes lead to heat generation. Sudden changes in the lattice distortion, due to magnetostriction, create lattice waves that carry off some of the energy. Sudden changes in the magnetization induce eddy currents that dissipate energy via Joule heating (domains have a finite electrical resistance). These processes involve energy conversion to heat and are irreversible. Sudden jerks in the wall motions lead to small jumps in the magnetization of the specimen as the magnetizing field is increased; the phenomenon is known as the **Barkhausen effect.** If we could examine the magnetization precisely with a highly sensitive instrument, we would see jumps in the M versus H behavior, as shown in the inset in Figure 8.31.

As we increase the field, magnetization continues to increase by jerky domain wall motions that enlarge domains with favorably oriented magnetizations and shrink away those with magnetizations pointing away from the applied field. Eventually domain wall motions leave each crystal grain with a single domain and magnetization in one of the easy directions, as indicated by point c in Figure 8.31. Although some grains would be oriented to have the easy direction and hence M along the applied field, the magnetization in many grains will be pointing at some angle to H as shown for point c in Figure 8.31. From then until point d, the increase in the applied field forces the magnetization in a grain, such as that at point c to rotate toward the direction of H. Eventually the applied field is sufficiently strong to align M along H, and the specimen reaches saturation magnetization M_{sat}, directed along H or $+x$, as at point d in Figure 8.31.

If we were to decrease and remove the magnetizing field, the magnetization in each grain would rotate to align parallel with the nearest easy direction in that grain. Further, in some grains, additional small domains may develop that reduce the magnetization within that grain, as indicated at point e in Figure 8.31. This process, from point d to point e, leaves the specimen with a permanent magnetization, called the **remanent** or **residual magnetization** and denoted by M_r.

If we were now to apply a magnetizing field in the reverse direction $-x$, the magnetization of the specimen, still along $+x$, would decrease and eventually, at a sufficiently large applied field M would be zero and the sample would have been totally demagnetized. This is shown as point f in Figure 8.31. The magnetizing field H_c required to totally demagnetize the sample is called the **coercivity** or the **coercive field.** It represents the resistance of the sample to demagnetization. We should note that at point f in Figure 8.31, the sample again has grains with many domains, which means that during the demagnetization process, from point e to point f, new domains had to be generated. The demagnetization process invariably involves the nucleation of various domains at various crystal imperfections to cancel the overall magnetization. The treatment of the nucleation of domains is beyond the scope of this book; we will nonetheless, accept it as required process for the demagnetization of the crystal grains.

If we continue to increase the applied magnetic field along $-x$, as illustrated in Figure 8.32a, the process from point f onward becomes similar to that described for magnetization from point a to point d in Figure 8.31 along $+x$ except that it is now directed along $-x$. At point g, the sample reaches saturation magnetization along the $-x$ direction. The full M versus H behavior as the magnetizing field is cycled between

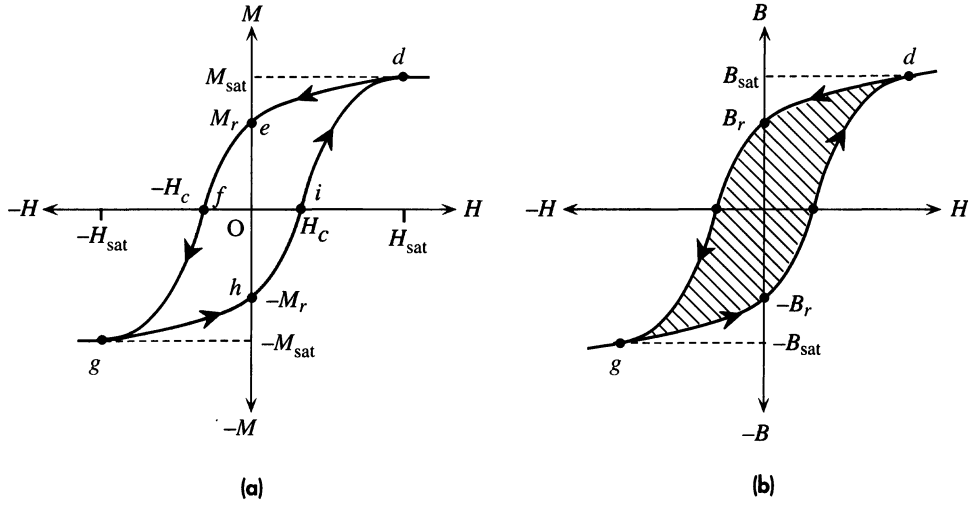

Figure 8.32

(a) A typical M versus H hysteresis curve.

(b) The corresponding B versus H hysteresis curve. The shaded area inside the hysteresis loop is the energy loss per unit volume per cycle.

$+x$ to $-x$ has a closed loop shape, shown in Figure 8.32a, called the **hysteresis loop.** We observe that in both $+x$ and $-x$ directions, the magnetization reaches saturation M_{sat} when H reaches H_{sat}, and on removing the applied field, the specimen retains an amount of permanent magnetization, represented by points e and h and denoted by M_r. The necessary applied field of magnitude H_c that is needed to demagnetize the specimen is the coercivity (or coercive field), which is represented by points f and i. The initial magnetization curve, $Oabcd$ in Figure 8.31, which starts from an unmagnetized state, is called the **initial magnetization curve.**

We can, of course, monitor the magnetic field B instead of M, as in Figure 8.32b, where

$$B = \mu_o M + \mu_o H$$

which leads to a hysteresis loop in the B versus H behavior. The very slight increase in B with H when M is in saturation is due to the permeability of free space ($\mu_o H$). The area enclosed within the B versus H hysteresis loop, shown as the hatched region in Figure 8.32b, represents the energy dissipated per unit volume per cycle of applied field variation.

Suppose we do not take a magnetic material to saturation but still subject the specimen to a cyclic applied field alternating between the $+x$ and $-x$ directions. Then the hysteresis loop would be different than that when the sample is taken all the way to saturation, as shown in Figure 8.33. The magnetic field in the material does not reach B_{sat} (corresponding to M_{sat}) but instead reaches some maximum value B_m when the magnetizing field is H_m. There is still a hysteresis effect because the magnetization and demagnetization processes are nonreversible and do not retrace each other. The shape of the hysteresis

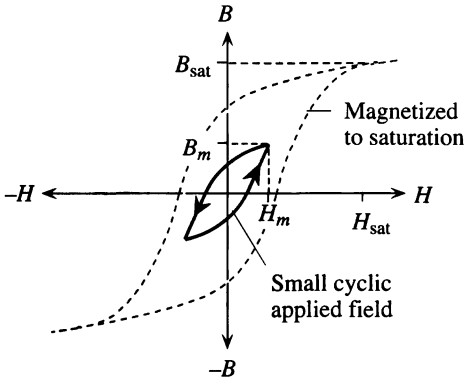

Figure 8.33 The *B* versus *H* hysteresis loop depends on the magnitude of the applied field in addition to the material and sample shape and size.

loop depends on the magnitude of the applied field in addition to the material and sample shape and size. The area enclosed within the loop is still the energy dissipated per unit volume per cycle of applied field oscillation. The hysteresis loop taken to saturation, as in Figure 8.32a and b, is called the **saturation (major) hysteresis loop.** It is apparent from Figure 8.33 that the remanence and coercivity exhibited by the sample depend on the *B–H* loop. The quoted values normally correspond to the saturation hysteresis loop.

Ferrimagnetic materials exhibit properties that closely resemble those of ferromagnetic materials. One can again identify distinct magnetic domains and domain wall motions during magnetization and demagnetization that also lead to *B–H* hysteresis curves with the same characteristic parameters, namely, saturation magnetization (M_{sat} and B_{sat} at H_{sat}), remanence (M_r and B_r), coercivity (H_c), hysteresis loss, and so on.

8.5.7 DEMAGNETIZATION

The *B–H* hysteresis curves, as in Figure 8.32b, that are commonly given for magnetic materials represent *B* versus *H* behavior observed under repeated cycling. The applied field intensity *H* is cycled back and forward between the $-x$ and $+x$ directions. If we were to try and demagnetize a specimen with a remanent magnetization at point *e* in Figure 8.34 by applying a reverse field intensity, then the magnetization would move along from point *e* to point *f*. If at point *f* we were to suddenly switch off the applied field, we would find that *B* does not actually remain zero but recovers along *f* to point e' and attains some value B_r'. The main reason is that small domain wall motions are reversible and as soon as the field is removed, there is some reversible domain wall motion "bouncing back" the magnetization along *f–e'*. We can anticipate this recovery and remove the field intensity at some point f' so that the sample recovers along f'O and the magnetization ends up being zero. However, to remove the field intensity at point f', we need to know not only the exact *B–H* behavior but also the exact location of point f' (or the recovery behavior). The simplest method to demagnetize the sample is first to cycle *H* with ample magnitude to reach saturation and then to continue cycling *H* but with a gradually decreasing magnitude, as depicted in Figure 8.35. As *H* is cycled with a decreasing magnitude, the sample traces out smaller and smaller *B–H* loops until the *B–H* loops are so small that they end up at the origin when *H* reaches

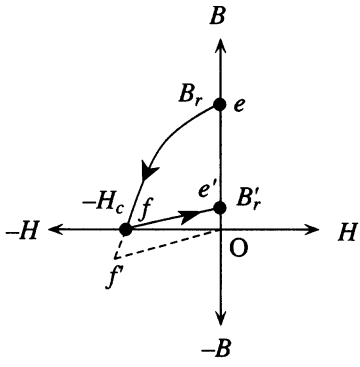

Figure 8.34 Removal of the demagnetizing field at point *f* does not necessarily result in zero magnetization as the sample recovers along *f*–*e*′.

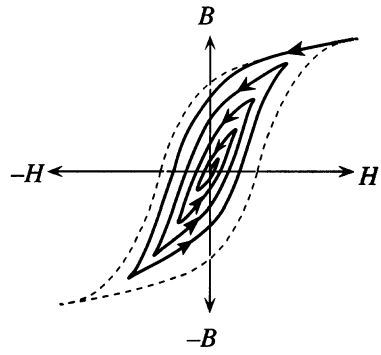

Figure 8.35 A magnetized specimen can be demagnetized by cycling the field intensity with a decreasing magnitude, that is, tracing out smaller and smaller *B*–*H* loops until the origin is reached, $H = 0$.

zero. The demagnetization process in Figure 8.35 is commonly known as **deperming.** Undesirable magnetization of various magnetic devices such as recording heads is typically removed by this deperming process (for example, a demagnetizing gun brought close to a magnetized recording head implements deperming by applying a cycled H with decreasing magnitude).

EXAMPLE 8.5 **ENERGY DISSIPATED PER UNIT VOLUME AND THE HYSTERESIS LOOP** Consider a toroidal coil with an iron core that is energized from a voltage supply through a rheostat, as shown in Figure 8.11. Suppose that by adjusting the rheostat we can adjust the current i supplied to the coil and hence the magnetizing field H in the core material. H and i are simply related by Ampere's law. However, the magnetic field B in the core is determined by the B–H characteristics of the core material. From electromagnetism (see Example 8.2), we know that the battery has to do work dE_{vol} per unit volume of core material to increase the magnetic field by dB, where

$$dE_{\text{vol}} = H\, dB$$

so that the total energy or work involved per unit volume in changing the magnetic field from an initial value B_1 to a final value B_2 in the core is

Work done per unit volume during magnetization

$$E_{\text{vol}} = \int_{B_1}^{B_2} H\, dB \qquad [8.22]$$

where the integration limits are determined by the initial and final magnetic fields.

Equation 8.22 corresponds to the area between the B–H curve and the B axis between B_1 and B_2. Suppose that we take the iron core in the toroid from point P on the hysteresis curve to Q, as shown in Figure 8.36. This is a magnetization process for which energy is put into the sample. The work done per unit volume from P to Q is the area $PQRS$, shown as hatched. On returning the sample to the same initial magnetization (same magnetic field B as we had at P), taking it from Q to S, energy is returned from the core into the electric circuit. This energy per unit volume is the area QRS, shown as gray, and is less than $PQRS$ during magnetization. The difference is the energy dissipated in the sample as heat (moving domain walls and so on) and

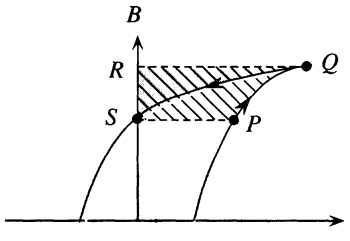

Figure 8.36 The area between the *B–H* curve and the *B* axis is the energy absorbed per unit volume in magnetization or released during demagnetization.

corresponds to the hysteresis loop area *PQS*. Over one full cycle, the energy dissipated per unit volume is the total hysteresis loop area.

The hysteresis loop and hence the energy dissipated per unit volume per cycle depend not only on the core material but also on the magnitude of the magnetic field (B_m), as apparent in Figure 8.33. For example, for magnetic steels used in transformer cores, the hysteresis **power loss** P_h per unit volume of core is empirically expressed in terms of the maximum magnetic field B_m and the ac frequency f as[6]

Hysteresis power loss per m³

$$P_h = KfB_m^n \qquad [8.23]$$

where K is a constant that depends on the core material (typically, $K = 150.7$), f is the ac frequency (Hz), B_m is the maximum magnetic field (T) in the core (assumed to be in the range 0.1–1.5 T), and $n = 1.6$. According to Equation 8.23, the hysteresis loss can be decreased by operating the transformer with a reduced magnetic field.

8.6 SOFT AND HARD MAGNETIC MATERIALS

8.6.1 DEFINITIONS

Based on their *B–H* behavior, engineering materials are typically classified into soft and hard magnetic materials. Their typical *B–H* hysteresis curves are shown in Figure 8.37. Soft magnetic materials are easy to magnetize and demagnetize and hence require relatively low magnetic field intensities. Put differently, their *B–H* loops are narrow, as shown in Figure 8.37. The hysteresis loop has a small area, so the hysteresis power loss per cycle is small. Soft magnetic materials are typically suitable for applications where repeated cycles of magnetization and demagnetization are involved, as in electric motors, transformers, and inductors, where the magnetic field varies cyclically. These applications also require low hysteresis losses, or small hysteresis loop area. Electromagnetic relays that have to be turned on and off require the relay iron to be magnetized and demagnetized and therefore need soft magnetic materials.

Hard magnetic materials, on the other hand, are difficult to magnetize and demagnetize and hence require relatively large magnetic field intensities, as apparent in Figure 8.37. Their *B–H* curves are broad and almost rectangular. They possess relatively large coercivities, which means that they need large applied fields to be demagnetized. The coercive field for hard materials can be millions of times greater than those for soft

[6] This is the power engineers Steinmetz equation for commercial magnetic steels. It has been applied not only to silicon irons (Fe + few percent Si) but also to a wide range of magnetic materials.

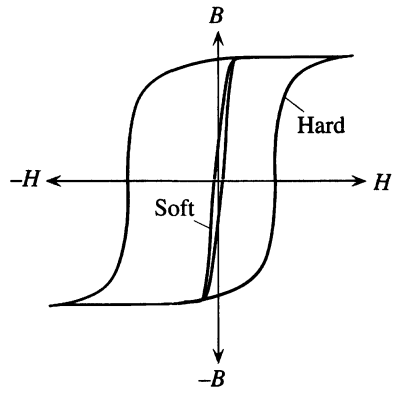

Figure 8.37 Soft and hard magnetic materials.

magnetic materials. Their characteristics make hard magnetic materials useful as permanent magnets in a variety of applications. It is also clear that the magnetization can be switched from one very persistent direction to another very persistent direction, from $+B_r$ to $-B_r$, by a suitably large magnetizing field intensity. As the coercivity is strong, both the states $+B_r$ and $-B_r$ persist until a suitable (large) magnetic field intensity switches the field from one direction to the other. It is apparent that hard magnetic materials can also be used in magnetic storage of digital data, where the states $+B_r$ and $-B_r$ can be made to represent 1 and 0 (or vice versa).

8.6.2 INITIAL AND MAXIMUM PERMEABILITY

It is useful to characterize the magnetization of a material by a relative permeability μ_r, since this simplifies magnetic calculations. For example, inductance calculations become straightforward if one could represent the magnetic material by μ_r alone. But it is clear from Figure 8.38a that

$$\mu_r = \frac{B}{\mu_o H}$$

is not even approximately constant because it depends on the applied field and the magnetic history of the sample. Nonetheless, we still find it useful to specify a relative permeability to compare various materials and even use it in various calculations. The definition $\mu_r = B/(\mu_o H)$ represents the slope of the straight line from the origin O to the point P, as shown in Figure 8.38a. This is a maximum when the line becomes a tangent to the B–H curve at P, as in the figure. Any other line from O to the B–H curve that is not a tangent does not yield a maximum relative permeability (the mathematical proof is left to the reader, though the argument is intuitively acceptable from the figure). The **maximum relative permeability,** as defined in Figure 8.38a, is denoted by $\mu_{r,\max}$ and serves as a useful magnetic parameter. The point P in Figure 8.38a that defines the maximum permeability corresponds to what is called the "knee" of the B–H curve. Many transformers are designed to operate with the maximum magnetic field in the core reaching this knee point. For pure iron, $\mu_{r,\max}$ is less than 10^4, but for certain

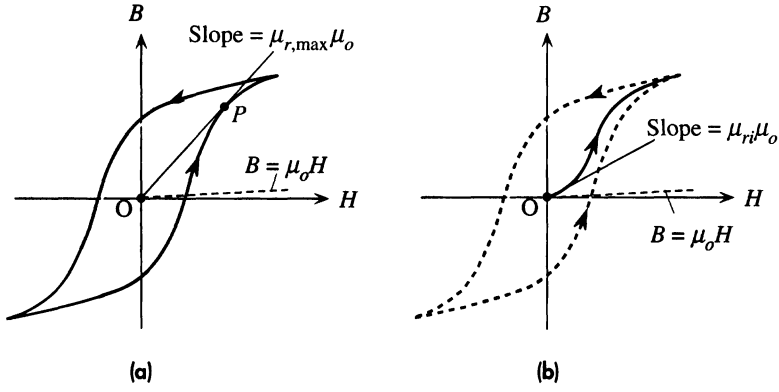

Figure 8.38 Definitions of (a) maximum permeability and (b) initial permeability.

soft magnetic materials such as supermalloys (a nickel–iron alloy), the values of $\mu_{r,\max}$ can be as high as 10^6.

Initial relative permeability, denoted as μ_{ri}, represents the initial slope of the initial B versus H curve as the material is first magnetized from an unmagnetized state, as illustrated in Figure 8.38b. This definition is useful for soft magnetic materials that are employed at very low magnetic fields (*e.g.*, small signals in electronics and communications engineering). In practice, weak applied magnetic fields where μ_{ri} is useful are typically less than 10^{-4} T. In contrast, $\mu_{r,\max}$ is useful when the magnetic field in the material is not far removed from saturation. Initial relative permeability of a magnetically soft material can vary by orders of magnitude. For example, μ_{ri} for iron is 150, whereas for supernumetal-200, a commercial alloy of nickel and iron, it is about 2×10^5.

8.7 SOFT MAGNETIC MATERIALS: EXAMPLES AND USES

Table 8.5 identifies what properties are desirable in soft magnetic materials and also lists some typical examples with various applications. An *ideal* soft magnetic material would have zero coercivity (H_c), a very large saturation magnetization (B_{sat}), zero remanent magnetization (B_r), zero hysteresis loss, and very large $\mu_{r,\max}$ and μ_{ri}. A number of example materials, from pure iron to ferrites, which are ferrimagnetic, are listed in Table 8.5. Pure iron, although soft, is normally not used in electric machines (except in a few specific relay-type applications) because its good conductivity allows large eddy currents to be induced under varying fields. Induced eddy currents in the iron lead to Joule losses (RI^2), which are undesirable. The addition of a few percentages of silicon to iron (silicon–iron), known typically as silicon–steels, increases the resistivity and hence reduces the eddy current losses. Silicon–iron is widely used in power transformers and electric machinery.

The nickle–iron alloys with compositions around 77% Ni–23% Fe constitute an important class of soft magnetic materials with low coercivity, low hysteresis losses, and high permeabilities (μ_{ri} and $\mu_{r,\max}$). High μ_{ri} makes these alloys particularly useful in low magnetic field applications that are typically found in high-frequency work in

Table 8.5 Selected soft magnetic materials and some typical values and applications

Magnetic Material	$\mu_o H_c$ (T)	B_{sat} (T)	B_r (T)	μ_{ri}	$\mu_{r,max}$	W_h	Typical Applications
Ideal soft	0	Large	0	Large	Large	0	Transformer cores, inductors, electric machines, electromagnet cores, relays, magnetic recording heads.
Iron (commercial) grade, 0.2% impurities)	$<10^{-4}$	2.2	<0.1	150	10^4	250	Large eddy current losses. Generally not preferred in electric machinery except in some specific applications (*e.g.*, some electromagnets and relays).
Silicon iron (Fe: 2–4% Si)	$<10^{-4}$	2.0	0.5–1	10^3	10^4–4×10^5	30–100	Higher resistivity and hence lower eddy current losses. Wide range of electric machinery (*e.g.*, transformers).
Supermalloy (79% Ni–15.5% Fe–5% Mo–0.5% Mn)	2×10^{-7}	0.7–0.8	<0.1	10^5	10^6	<0.5	High permeability, low-loss electric devices, *e.g.*, specialty transformers, magnetic amplifiers.
78 Permalloy (78.5% Ni–21.5% Fe)	5×10^{-6}	0.86	<0.1	8×10^3	10^5	<0.1	Low-loss electric devices, audio transformers, HF transformers, recording heads, filters.
Glassy metals, Fe–Si–B	2×10^{-6}	1.6	$<10^{-6}$	—	10^5	20	Low-loss transformer cores.
Ferrites, Mn–Zn ferrite	10^{-5}	0.4	<0.01	2×10^3	5×10^3	<0.01	HF low-loss applications. Low conductivity ensures negligible eddy current losses. HF transformers, inductors (*e.g.*, pot cores, E and U cores), recording heads.

NOTE: W_h is the hysteresis loss, energy dissipated per unit volume per cycle in hysteresis losses, J m^{-3} cycle^{-1}, typically at $B_m = 1$ T.

electronics (*e.g.*, audio and wide-band transformers). They have found many engineering uses in sensitive relays, pulse and wide-band transformers, current transformers, magnetic recording heads, magnetic shielding, and so forth. Alloying iron with nickel increases the resistivity and hence reduces eddy current losses. The magnetocrystalline anisotropy energy is least at these nickel compositions, which leads to easier domain wall motions and hence smaller hysteresis losses. There are a number of commercial nickel–iron alloys whose application depends on the exact composition (which may also have a few percentages of Mo, Cu, or Cr) and the method of preparation (*e.g.*, mechanical rolling). For example, supermalloy (79% Ni–16% Fe–5% Co) has $\mu_{ri} \approx 10^5$, compared with commercial grade iron, which has μ_{ri} less than 10^3.

Amorphous magnetic metals, as the name implies, have no crystal structure (they only have short-range order) and consequently possess no crystalline imperfections such as grain boundaries and dislocations. They are prepared by rapid solidification of the melt by using special techniques such as melt spinning (as described in Chapter 1). Typically they are thin ribbons by virtue of their preparation method. Since they have no crystal structure, they also have no magnetocrystalline anisotropy energy, which means that all

directions are easy. The absence of magnetocrystalline anisotropy and usual crystalline defects which normally impede domain wall motions, leads to low coercivities and hence to soft magnetic properties. The coercivity, however, is not zero inasmuch as there is still some magnetic anisotropy due to the directional nature of the strains frozen in the metal during rapid solidification. By virtue of their disordered structure, these metallic glasses also have higher resistivities and hence they have smaller eddy current losses. Although they are ideally suited for various transformer and electric machinery applications, their limited size and shape, at present, prevent their use in power applications.

Ferrites are ferrimagnetic materials that are typically oxides of mixed transition metals, one of which is iron. For example, Mn ferrite is $MnFe_2O_4$ and MgZn ferrite is $Mn_{1-x}Zn_xFe_2O_4$. They are normally insulators and therefore do not suffer from eddy current losses. They are ideal as magnetic materials for high-frequency work where eddy current losses would prevent the use of any material with a reasonable conductivity. Although they can have high initial permeabilities and low losses, they do not possess as large saturation magnetizations as ferromagnets, and further, their useful temperature range (determined by the Curie temperature) is lower. There are many types of commercial ferrites available depending on the application, tolerable losses, and the required upper frequency of operation. MnZn ferrites, for example, have high initial permeabilities (*e.g.*, 2×10^3) but are only useful up to about 1 MHz, whereas NiZn ferrites have lower initial permeability (*e.g.*, 10^2) but can be used up to 200 MHz. Generally, the initial permeability in the high-frequency region decreases with frequency.

Garnets are ferrimagnetic materials that are typically used at the highest frequencies that cover the microwave range (1–300 GHz). The yttrium iron garnet, YIG, which is $Y_3Fe_5O_{12}$, is one of the simplest garnets with a very low hysteresis loss at microwave frequencies. Garnets have excellent dielectric properties with high resistivities and hence low losses. The main disadvantages are the low saturation magnetization, which is 0.18 T for YIG, and low Curie temperature, 280 °C for YIG. The compositions of garnets depend on the properties required for the particular microwave application. For example, $Y_{2.1}Gd_{0.98}Fe_5O_{12}$ is a garnet that is used in X-band (8–12 GHz) three-port circulators handling high microwave powers (*e.g.*, peak power 200 kW and average power 200 W).

EXAMPLE 8.6

AN INDUCTOR WITH A FERRITE CORE Consider a toroidal coil with a ferrite core. Suppose that the coil has 200 turns and is used in HF work with small signals. The mean diameter of the toroid is 2.5 cm and the core diameter is 0.5 cm. If the core is a MnZn ferrite, what is the approximate inductance of the coil?

SOLUTION

The inductance L of a toroidal coil is given by

$$L = \frac{\mu_{ri}\mu_o N^2 A}{\ell}$$

so

$$L = \frac{(2 \times 10^3)(4\pi \times 10^{-7}\,\mathrm{H\,m^{-1}})(200)^2\pi\left(\frac{0.005}{2}\,\mathrm{m}\right)^2}{(\pi 0.025\,\mathrm{m})} = 0.025\ \mathrm{H} \quad \text{or} \quad 25\ \mathrm{mH}$$

Had the core been air, the inductance would have been 1.26×10^{-5} H or 12.6 μH. The main assumption is that B is uniform in the core, and this will be only so if the diameter of the toroid (2.5 cm) is much greater than the core diameter (0.5 cm). Here this ratio is 5 and the calculation is only approximate.

8.8 HARD MAGNETIC MATERIALS: EXAMPLES AND USES

An ideal hard magnetic material, as summarized in Table 8.6, has very large coercivity and remanent magnetic field. Further, since they are used as permanent magnets, the energy stored per unit volume in the external magnetic field should be as large as possible since this is the energy available to do work. This energy density (J m^{-3}) in the external field depends on the maximum value of the product BH in the second quadrant of the B–H characteristics and is denoted as $(BH)_{max}$. It corresponds to the largest rectangular area that fits the B–H curve in the second quadrant, as shown in Figure 8.39.

When the size of a ferromagnetic sample falls below a certain critical dimension, of the order of 0.1 μm for cobalt, the whole sample becomes a single domain, as depicted in Figure 8.40, because the cost of energy in generating a domain wall is too high compared with the reduction in external magnetostatic energy. These small particle-like pieces of magnets are called **single domain fine particles.** Their magnetic

Table 8.6 Hard magnetic materials and typical values

Magnetic Material	$\mu_o H_c$ (T)	B_r (T)	$(BH)_{max}$ (kJ m^{-3})	Examples and Uses
Ideal hard	Large	Large	Large	Permanent magnets in various applications.
Alnico (Fe–Al–Ni–Co–Cu)	0.19	0.9	50	Wide range of permanent magnet applications.
Alnico (Columnar)	0.075	1.35	60	
Strontium ferrite (anisotropic)	0.3–0.4	0.36–0.43	24–34	Starter motors, dc motors, loudspeakers, telephone receivers, various toys.
Rare earth cobalt, *e.g.*, Sm_2Co_{17} (sintered)	0.62–1.1	1.1	150–240	Servo motors, stepper motors, couplings, clutches, quality audio headphones.
NdFeB magnets	0.9–1.0	1.0–1.2	200–275	Wide range of applications, small motors (*e.g.*, in hand tools), walkman equipment, CD motors, MRI body scanners, computer applications.
Hard particles, γ-Fe_2O_3	0.03	0.2		Audio and video tapes, floppy disks.

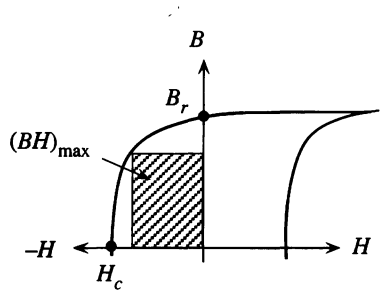

Figure 8.39 Hard magnetic materials and $(BH)_{max}$.

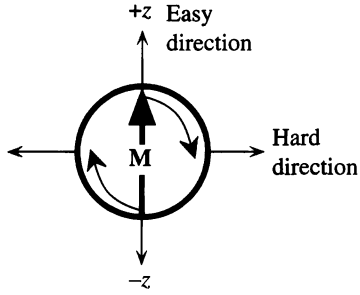

Figure 8.40 A single domain fine particle.

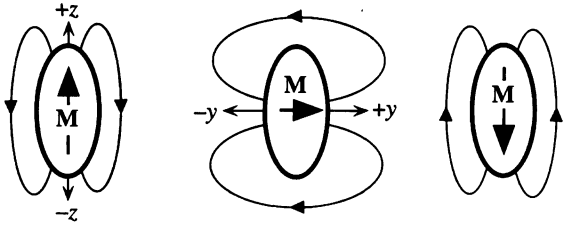

Figure 8.41 A single domain elongated particle. Due to shape anisotropy, magnetization prefers to be along the long axis as in (a). Work has to be done to change **M** from (a) to (b) to (c).

properties depend not only on the crystal structure of the particle but also on the shape of the particle because different shapes give rise to different external magnetic fields. For a spherical iron particle, the magnetization **M** will be in an easy direction, for example, along [100] taken along $+z$. To reverse the magnetization from $+z$ to $-z$ by an applied field, we have to rotate the spins around past the hard direction, as shown in Figure 8.40, since we cannot generate reverse domains (or move domain walls). The rotation of magnetization involves substantial work due to the magnetocrystalline anisotropic energy, and the result is high coercivity. The higher the magnetocrystalline anisotropy energy, the greater the coercivity. The energy involved in creating a domain wall increases with the magnetocrystalline anisotropy energy. The critical size below which a particle becomes a single domain therefore increases with the crystalline anisotropy. Barium ferrite crystals have the hexagonal structure and hence have a high degree of magnetocrystalline anisotropy. Critical size for single domain barium ferrite particles is about 1–1.5 μm, and the coercivity $\mu_o H_c$ of small particles can be as high as 0.3 T, compared with values 0.02–0.1 T in multidomain barium ferrite pieces.

Particles that are not spherical may even have higher coercivity as a result of shape anisotropy. Consider an ellipsoid (elongated) fine particle, shown in Figure 8.41a. If the magnetization **M** is along the long axis (along z), then the potential energy in the external magnetic field is less than if **M** were along the minor axis (along y), as compared in Figure 8.41a and b. Thus, we have to do work to rotate **M** from the long to the short axis, or from Figure 8.41a to b. An elongated fine particle therefore has its magnetization along its length, and the effect is called **shape anisotropy.** If we have to

reverse the magnetization from $+z$ to $-z$ by applying a reverse field, then we can only do so by rotating the magnetization, as shown in Figure 8.41a to c. **M** has to be rotated around through the minor axis, and this involves substantial work. Thus the coercivity is high. In general, the greater the elongation of the particle with respect to its width, the higher the coercivity. Small spherical Fe–Cr–Co particles have a coercivity $\mu_o H_c$ at most 0.02 T, but elongated and aligned particles can have a coercivity as high as 0.075 T due to shape anisotropy.

High coercivity magnets can be fabricated by having elongated fine particles dispersed by precipitation in a structure. Fine particles will be single domains. Alnico is a popular permanent magnet material that is an alloy of the metals Al, Ni, Co, and Fe (hence the name). Its microstructure consists of fine elongated Fe–Co rich particles, called the α'-phase, dispersed in a matrix that is Ni–Al rich and called the α-phase. The structure is obtained by an appropriate heat treatment that allows fine α' particles to precipitate out from a solid solution of the alloy. The α' particles are strongly magnetic, whereas the α-phase matrix is weakly magnetic. When the heat treatment is carried out in the presence of a strong applied magnetic field, the α' particles that are formed have their elongations (or lengths) and hence their magnetizations along the applied field. The demagnetization process requires the rotations of the magnetizations in single domain elongated α' particles, which is a difficult process (shape anisotropy), and hence the coercivity is high. The main drawback of the Alnico magnet is that the alloy is mechanically hard and brittle and cannot be shaped except by casting or sintering before heat treatment. There are, however, other alloy permanent magnets that can be machined.

A variety of permanent magnets are made by compacting high-coercivity particles by using powder metallurgy (*e.g.*, powder pressing or sintering). The particles are magnetically hard because they are sufficiently small for each to be of single domain or they possess substantial shape anisotropy (elongated particles may be ferromagnetic alloys, *e.g.*, Fe–Co, or various hard ferrites). These are generically called powdered solid permanent magnets. An important class is the **ceramic magnets** that are made by compacting barium ferrite, $BaFe_{12}O_9$, or strontium ferrite, $SrFe_{12}O_9$, particles. The barium ferrite has the hexagonal crystal structure with a large magnetocrystalline anisotropy, which means that barium ferrite particles have high coercivity. The ceramic magnet is typically formed by wet pressing ferrite powder in the presence of a magnetizing field, which allows the easy directions of the particles to be aligned, and then drying and carefully sintering the ceramic. They are used in many low-cost applications.

Rare earth cobalt permanent magnets based on samarium–cobalt (Sm–Co) alloys have very high $(BH)_{max}$ values and are widely used in many applications such as dc motors, stepper and servo motors, traveling wave tubes, klystrons, and gyroscopes. The intermetallic compound $SmCo_5$ has a hexagonal crystal structure with high magnetocrystalline anisotropy and hence high coercivity. The $SmCo_5$ powder is pressed in the presence of an applied magnetic field to align the magnetizations of the particles. This is followed by careful sintering to produce a solid powder magnet. The Sm_2Co_{15} magnets are more recent and have particularly high values of $(BH)_{max}$ up to about 240 kJ m^{-3}. Sm_2Co_{15} is actually a generic name and the alloy may contain other transition metals substituting for some of the Co atoms.

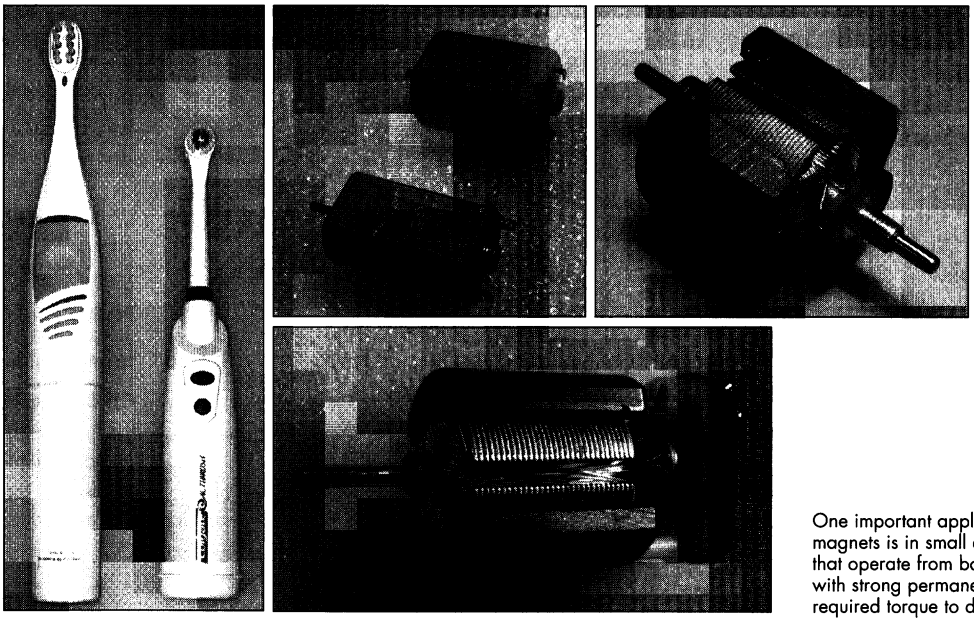

One important application of permanent magnets is in small dc motors. Toothbrushes that operate from batteries use dc motors with strong permanent magnets to get the required torque to drive the brushes.

The more recent **neodymium–iron–boron,** NdFeB, powdered solid magnets can have very large $(HB)_{max}$ values up to about 275 kJ m^{-3}. The tetragonal crystal structure has the easy direction along the long axis and possesses high magnetocrystalline anisotropic energy. This means that we need a substantial amount of work to rotate the magnetization around through the hard direction, and hence the coercivity is also high. The main drawback is the lower Curie temperature, typically around 300 °C, whereas for Alnico and rare earth cobalt magnets, the Curie temperatures are above 700 °C. Another method of preparing NdFeB magnets is by the recrystallization of amorphous NdFeB at an elevated temperature in an applied field. The grains in the recrystallized structure are sufficiently small to be single domain grains and therefore possess high coercivity.

EXAMPLE 8.7

$(BH)_{max}$ FOR A PERMANENT MAGNET Consider the permanent magnet in Figure 8.42. There is a small air gap of length ℓ_g where there is an external magnetic field that is available to do work. For example, if we were to insert an appropriate coil in the gap and pass a current through the coil, it would rotate as in a moving coil panel meter. Show that the magnetic energy per unit volume stored in the gap is proportional to the maximum value of BH. How does $(BH)_{max}$ vary with the magnetizing field?

SOLUTION

Let ℓ_m be the mean length of the magnet from one end to the other, as shown in Figure 8.42. We assume that the cross-sectional area A is constant throughout. There are no windings around the magnet and no current, $I = 0$. Ampere's law for H involves integrating H along a closed path or around the mean path length $\ell_m + \ell_g$. Suppose that H_m and H_g are the magnetic

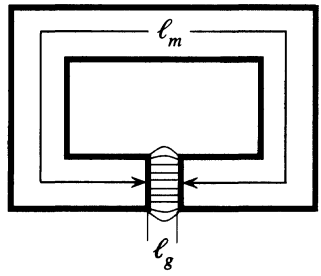

Figure 8.42 A permanent magnet with a small air gap.

field intensities in the permanent magnet and in the gap, respectively. Then $H\,d\ell$ integrated around $\ell_m + \ell_g$ is

$$\oint H\,d\ell = H_m\ell_m + H_g\ell_g = 0$$

so that

$$H_g = -H_m\frac{\ell_m}{\ell_g}$$

and hence

B–H for air gap

$$B_g = -\mu_o\frac{\ell_m}{\ell_g}H_m \qquad \textbf{[8.24]}$$

Equation 8.24 is a relationship between B_g in the gap and H_m in the magnet. In addition, we have the *B–H* relationship for the magnetic material itself between the magnetic field B_m and intensity H_m in the magnet, that is,

B–H for magnet material

$$B_m = f(H_m) \qquad \textbf{[8.25]}$$

The magnetic flux in the magnet and in the air gap must be continuous. Since we assumed a uniform cross-sectional area, the continuity of flux across the air gap implies that $B_m = B_g$. Thus we need to equate Equation 8.24 to Equation 8.25. Equation 8.24 is a straight line with a negative slope in a B_g versus H_m plot, as shown in Figure 8.43a. Equation 8.25 is, of course, the *B–H* characteristics of the material. The two intersect at point *P*, as shown in Figure 8.43a, where $B_g = B_m = B'_m$ and $H_m = H'_m$.

We know that there is magnetic energy in the air gap given by

$$\begin{aligned} E_{\text{mag}} &= (\text{Gap volume})(\text{Magnetic energy density in the gap}) \\ &= (A\ell_g)\left(\frac{1}{2}B_gH_g\right) = \frac{1}{2}(A\ell_g)B'_mH'_m\left(\frac{\ell_m}{\ell_g}\right) \\ &= \frac{1}{2}(A\ell_m)B'_mH'_m \\ &= \frac{1}{2}(\text{Magnet volume})B'_mH'_m \qquad \textbf{[8.26]} \end{aligned}$$

Energy in air gap of a magnet

Thus, the external magnetic energy depends on the magnet volume and the *product* of B'_m and H'_m of the magnet characteristics at the operating point *P*. For a given magnet size, the magnetic energy in the gap is proportional to the rectangular area $B'_mH'_m$, $OB'_mPH'_m$ in Figure 8.43a,

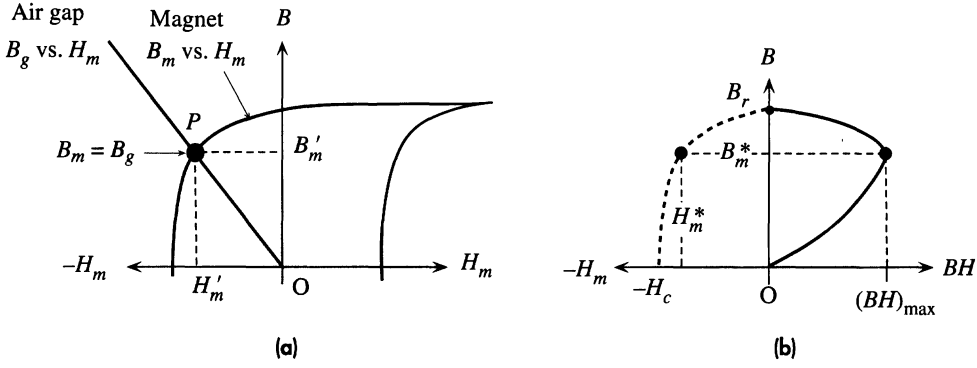

Figure 8.43

(a) Point *P* represents the operating point of the magnet and determines the magnetic field inside and outside the magnet.

(b) Energy density in the gap is proportional to *BH*, and for a given geometry and size of gap, this is a maximum at a particular magnetic field B^*_m or B^*_g.

and we have to maximize this area for the best energy extraction. Figure 8.43b shows how the product BH varies with B in a typical magnetic material. BH is maximum at $(BH)_{max}$, when the magnetic field is B^*_m and the field intensity is H^*_m. We can appropriately choose the air-gap size to operate at these values, in which case we will be only limited by the $(BH)_{max}$ available for that magnetic material. It is clear that $(BH)_{max}$ is a good figure of merit for comparing hard magnetic materials. According to Table 8.6, we can extract four to five times more work from a rare earth cobalt magnet than from an Alnico magnet of the same size if we were not limited by economics and weight. It should be mentioned that Equation 8.26 is only approximate as it neglects all fringe fields.

8.9 SUPERCONDUCTIVITY

8.9.1 ZERO RESISTANCE AND THE MEISSNER EFFECT

In 1911 Kamerlingh Onnes at the University of Leiden in Holland observed that when a sample of mercury is cooled to below 4.2 K, its resistivity totally vanishes and the material behaves as a **superconductor,** exhibiting no resistance to current flow. Other experiments since then have shown that there are many such substances, not simply metals, that exhibit superconductivity when cooled below a **critical temperature** T_c that depends on the material. On the other hand, there are also many conductors, including some with the highest conductivities such as silver, gold, and copper, that do not exhibit superconductivity. The resistivity of these **normal conductors** at low temperatures is limited by scattering from impurities and crystal defects and saturates at a finite value determined by the residual resistivity. The two distinctly different types of behavior are depicted in Figure 8.44. Between 1911 and 1986, many different metals and metal alloys had been studied, and the highest

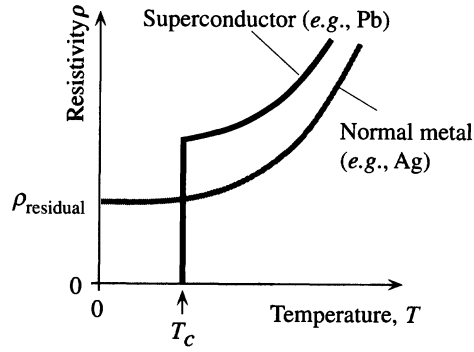

Figure 8.44 A superconductor such as lead evinces a transition to zero resistivity at a critical temperature T_c (7.2 K for Pb).
A normal conductor such as silver exhibits residual resistivity down to lowest temperatures.

recorded critical temperature was about 23 K in a niobium–germanium compound (Nb_3Ge) whose superconductivity was discovered in the early 1970s. In 1986 Bednorz and Müller, at IBM Research Laboratories in Zürich, discovered that a copper oxide–based ceramic-type compound La–Ba–Cu–O, which normally has high resistivity, becomes superconducting when cooled below 35 K. Following this Nobel prize–winning discovery, a variety of copper oxide–based compounds (called cuprate ceramics) have been synthesized and studied. In 1987 it was found that yttrium barium copper oxide (Y–Ba–Cu–O) becomes superconducting at a critical temperature of 95 K, which is above the boiling point of nitrogen (77 K). This discovery was particularly significant because liquid nitrogen is an inexpensive cryogent that is readily liquified and easy to use compared with cryogent liquids that had to be used in the

Superconductivity, zero resistance below a certain critical temperature, was discovered by a Dutch physicist, Heike Kamerlingh Onnes, in 1911. Kamerlingh Onnes and one of his graduate students found that the resistance of frozen mercury simply vanished at 4.15 K; Kamerlingh Onnes won the Nobel prize in 1913.

SOURCE: © Rijksmuseum voor de Geschiedenis der Natuurwetenschappen, courtesy AIP Emilio Segrè Visual Archives.

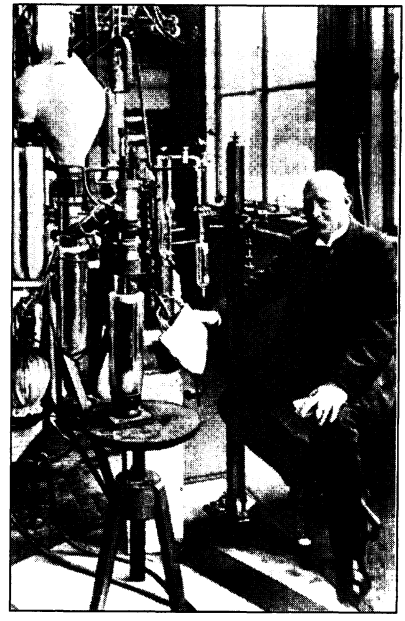

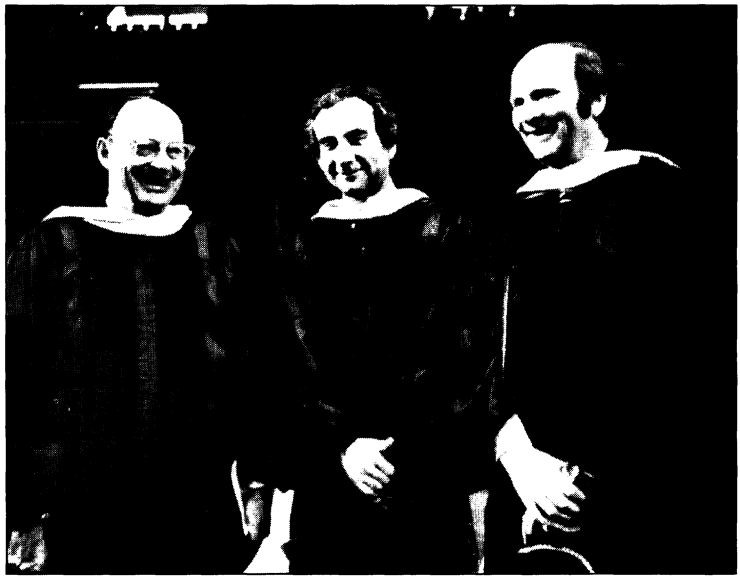

John Bardeen, Leon N. Cooper, and John Robert Schrieffer, in Nobel prize ceremony (1972). They received the Nobel prize for the explanation of superconductivity in terms of Cooper pairs.

SOURCE: AIP Emilio Segrè Visual Archives.

"My belief is that the pairing condensation is what Mother Nature had in mind when she created these fascinating high-T_c systems." Robert Schrieffer (1991)

past (liquid helium). At present the highest critical temperature for a superconductor is around 130 K (−143 °C) for Hg–Ba–Ca–Cu–O. These superconductors with T_c above ~30 K are now typically referred as **high-T_c superconductors.** The quest for a near-room-temperature superconductor goes on, with many scientists around the world trying different materials, or synthesizing them, to raise T_c even higher. There are already commercial devices utilizing high-T_c superconductors, for example, thin-film SQUIDs[7] that can accurately measure very small magnetic fluxes, high-Q filters, and resonant cavities in microwave communications.

The vanishing of resistivity is not the only characteristic of a superconductor. A superconductor cannot be viewed simply as a substance that has infinite conductivity below its critical temperature. A superconductor below its critical temperature expels all the magnetic field from the bulk of the sample as if it were a perfectly diamagnetic substance. This phenomenon is known as the **Meissner effect.** Suppose that we place a superconducting material in a magnetic field above T_c. The magnetic field lines will penetrate the sample, as we expect for any low μ_r medium. However, when the superconductor is cooled below T_c, it rejects all the magnetic flux in the sample, as depicted in Figure 8.45. The superconductor develops a magnetization M by developing surface currents, such that M and the applied field cancel everywhere inside

[7] SQUID is a superconducting quantum interference device that can detect very small magnetic fluxes.

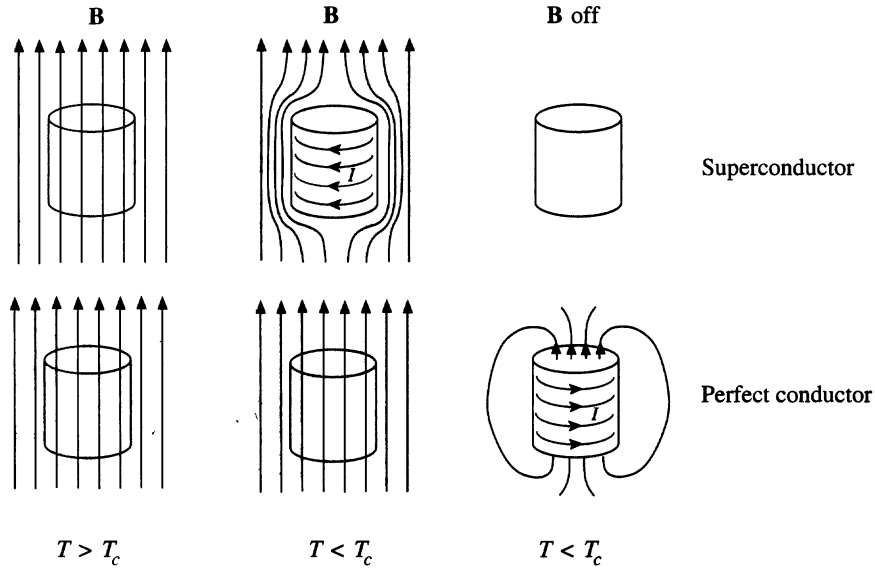

Figure 8.45 The Meissner effect.
A superconductor cooled below its critical temperature expels all magnetic field lines from the bulk by setting up a surface current. A perfect conductor ($\sigma = \infty$) shows no Meissner effect.

the sample. Put differently $\mu_o M$ is in the *opposite* direction to the applied field and equal to it in magnitude. Thus, below T_c a superconductor is a perfectly diamagnetic substance ($\chi_m = -1$). This should be contrasted with the behavior of a perfect conductor, which only exhibits infinite conductivity, or $\rho = 0$, below T_c. If we place a perfect conductor in a magnetic field and then cool it below T_c, the magnetic field is not rejected. These two types of behavior are identified in Figure 8.45. If we switch off the field, the field around the superconductor simply disappears. But switching off the field means there is a decreasing applied field. This change in the field induces currents in the perfect conductor by virtue of Faraday's law of induction. These currents generate a magnetic field that opposes the change (Lenz's law); in other words, they generate a field along the same direction as the applied field to reenforce the decreasing field. As the current can be sustained ($\rho = 0$) without Joule dissipation, it keeps on flowing and maintaining the magnetic field. The two final situations are shown in Figure 8.45 and distinguish the Meissner effect, a distinct characteristic of a superconductor, from the behavior of a perfect conductor ($\rho = 0$ only). The photograph showing the levitation of a magnet above the surface of a superconductor (Figure 8.46) is the direct result of the Meissner effect: the exclusion of the magnet's magnetic fields from the interior of the superconductor.

The transition from the normal state to the superconducting state as the temperature falls below the critical temperature has similarities with phase transitions such as solid to liquid or liquid to vapor changes. At the critical temperature, there is a sharp change in the heat capacity as one would observe for any phase change. In the superconducting

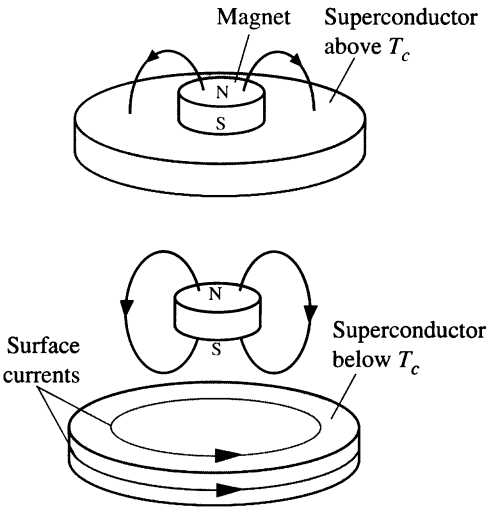

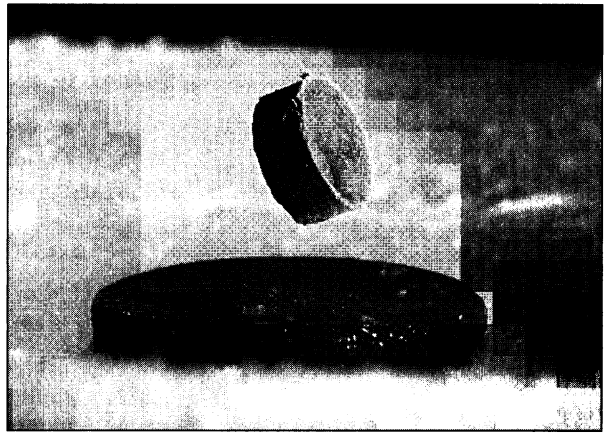

Figure 8.46

Left: A magnet over a superconductor becomes levitated. The superconductor is a perfect diamagnet which means that there can be no magnetic field inside the superconductor.

Right: Photograph of a magnet levitating above a superconductor immersed in liquid nitrogen (77 K). This is the Meissner effect.

| SOURCE: Photo courtesy of Professor Paul C. W. Chu.

state, we cannot treat a conduction electron in isolation. The electrons behave collectively and thereby impart the superconducting characteristics to the substance, as discussed later.

8.9.2 TYPE I AND TYPE II SUPERCONDUCTORS

The superconductivity below the critical temperature has been observed to disappear in the presence of an applied magnetic field exceeding a critical value denoted by B_c. This critical field depends on the temperature and is a characteristic of the material. Figure 8.47 shows the dependence of the critical field on the temperature. The critical field is maximum, $B_c(0)$, when $T = 0$ K (obtained by extrapolation[8]). As long as the applied field is below B_c at that temperature, the material is in the superconducting state, but when the field exceeds B_c, the material reverts to the normal state. We know that in the superconducting state, the applied magnetic field lines are expelled from the sample and the phenomenon is called the Meissner effect. The external field, in fact, does penetrate the sample from the surface into the bulk, but the magnitude of this penetrating field decreases exponentially from the surface. If the field at the surface of the sample is B_o, then at a distance x from the surface, the field is

[8] There is a third law to thermodynamics that is not as emphasized as the first two laws, which dominate all branches of engineering. That is, one can never reach the absolute zero of temperature.

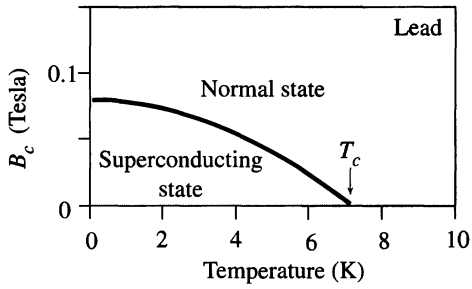

Figure 8.47 The critical field versus temperature in Type I superconductors.

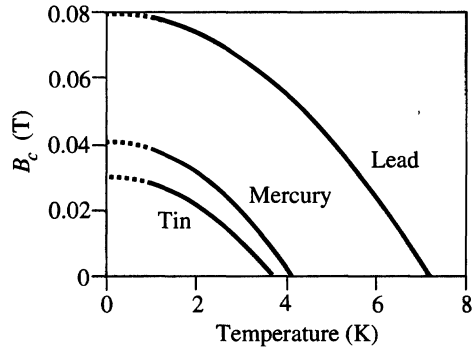

Figure 8.48 The critical field versus temperature in three examples of Type I superconductors.

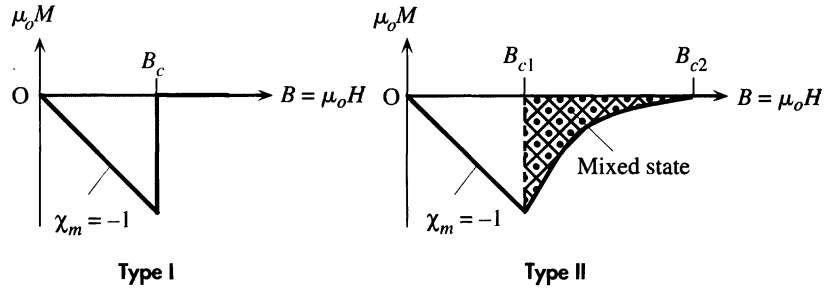

Figure 8.49 Characteristics of Type I and Type II superconductors. $B = \mu_o H$ is the applied field and M is the overall magnetization of the sample. Field inside the sample, $B_{\text{inside}} = \mu_o H + \mu_o M$, which is zero only for $B < B_c$ (Type I) and $B < B_{c1}$ (Type II).

given by an exponential decay,

$$B(x) = B_o \exp\left(-\frac{x}{\lambda}\right)$$

where λ is a "characteristic length" of penetration, called the **penetration depth,** and depends on the temperature and T_c (or the material). At the critical temperature, the penetration length is infinite and any magnetic field can penetrate the sample and destroy the superconducting state. Near absolute zero of temperature, however, typical penetration depths are 10–100 nm. Figure 8.48 shows the B_c versus T behavior for three example superconductors, tin, mercury, and lead.

Superconductors are classified into two types, called Type I and Type II, based on their diamagnetic properties. In Type I superconductors, as the applied magnetic field B increases, so does the opposing magnetization M until the field reaches the critical field B_c, whereupon the superconductivity disappears. At that point, the perfect diamagnetic behavior, the Meissner effect, is lost, as illustrated in Figure 8.49. A Type I superconductor below B_c is in the **Meissner state,** where it excludes all the magnetic

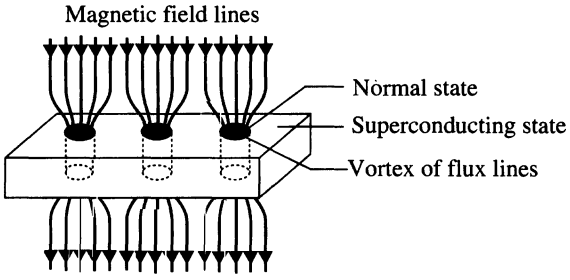

Figure 8.50 The mixed or vortex state in a Type II superconductor.

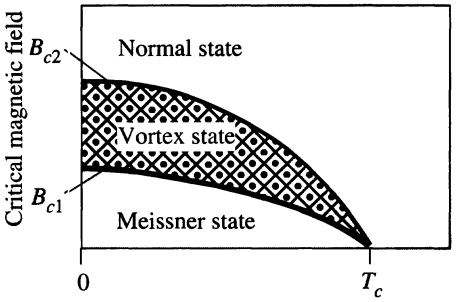

Figure 8.51 Temperature dependence of B_{c1} and B_{c2}.

flux from the interior of the sample. Above B_c it is in the normal state, where the magnetic flux penetrates the sample as it would normally and the conductivity is finite.

In the case of Type II superconductors, the transition does not occur sharply from the Meissner state to the normal state but goes through an intermediate phase in which the applied field is able to pierce through certain local regions of the sample. As the magnetic field increases, initially the sample behaves as a perfect diamagnet exhibiting the Meissner effect and rejecting all the magnetic flux. When the applied field increases beyond a critical field denoted as B_{c1}, the **lower critical field,** the magnetic flux lines are no longer totally expelled from the sample. The overall magnetization M in the sample opposes the field, but its magnitude does not cancel the field everywhere. As the field increases, M gets smaller and more flux lines pierce through the sample until at B_{c2}, the **upper critical field,** all field lines penetrate the sample and superconductivity disappears. This behavior is shown in Figure 8.49. Type II superconductors therefore have two critical fields B_{c1} and B_{c2}.

When the applied field is between B_{c1} and B_{c2}, the field lines pierce through the sample through tubular local regions, as pictured in Figure 8.50. The sample develops local small cylindrical (filamentary) regions of normal state in a matrix of superconducting state and the magnetic flux lines go though these filaments of local normal state, as shown in Figure 8.50. The state between B_{c1} and B_{c2} is called the **mixed state** (or **vortex state**) because there are two states—normal and superconducting—mixed in the same sample. The filaments of normal state have finite conductivity and a quantized amount of flux through them. Each filament is a **vortex** of flux lines (hence the name *vortex state*). It should be apparent that there should be currents circulating around the walls of vortices. These circulating currents ensure that the magnetic flux through the superconducting matrix is zero. The sample overall has infinite conductivity due to the superconducting regions. Figure 8.51 shows the dependence of B_{c1} and B_{c2} on the temperature and identifies the regions of Meissner, mixed, and normal states. All engineering applications of superconductors invariably use Type II materials because B_{c2} is typically much greater than B_c found in Type I materials and, furthermore, the critical temperatures of Type II materials are higher than those of Type I. Many superconductors, including the recent high-T_c superconductors, are of Type II. Table 8.7 summarizes the characteristics of selected Type I and Type II superconductors.

Table 8.7 Examples of Type I and Type II superconductors

Type I	Sn	Hg	Ta	V	Pb	Nb
T_c (K)	3.72	4.15	4.47	5.40	7.19	9.2
B_c (T)	0.030	0.041	0.083	0.14	0.08	0.198

Type II	Nb_3Sn	Nb_3Ge	$Ba_{2-x}Br_xCuO_4$	Y–Ba–Cu–O ($YBa_2Cu_3O_7$)	Bi–Sr–Ca–Cu–O ($Bi_2Sr_2Ca_2Cu_3O_{10}$)	Hg–Ba–Ca–Cu–O
T_c (K)	18.05	23.2	30–35	93–95	122	130–135
B_{c2} (Tesla) at 0 K	24.5	38	~150	~300		
J_c (A cm^{-2}) at 0 K	~10^7			10^4–10^7		

NOTE: Critical fields are close to absolute zero, obtained by extrapolation. Type I for pure, clean elements.

8.9.3 CRITICAL CURRENT DENSITY

Another important characteristic feature of the superconducting state is that when the current density through the sample exceeds a critical value J_c, it is found that superconductivity disappears. This is not surprising since the current through the superconductor will itself generate a magnetic field and at sufficiently high current densities, the magnetic field at the surface of the sample will exceed the critical field and extinguish superconductivity. This plausible direct relation between B_c and J_c is only true for Type I superconductors, whereas in Type II superconductors, J_c depends in a complicated way on the interaction between the current and the flux vortices. New high-T_c superconductors have exceedingly high critical fields, as apparent in Table 8.7, that do not seem to necessarily translate to high critical current densities. The critical current density in Type II superconductors depends not only on the temperature and the applied magnetic field but also on the preparation and hence the microstructure (*e.g.*, polycrystallinity) of the superconductor material. Critical current densities in new high-T_c superconductors vary widely with preparation conditions. For example, in Y–Ba–Cu–O, J_c may be greater than 10^7 A cm^{-2} in some carefully prepared thin films and single crystals but around 10^3–10^6 A cm^{-2} in some of the polycrystalline bulk material (*e.g.*, sintered bulk samples). In Nb_3Sn, used in superconducting solenoid magnets, on the other hand, J_c is close to 10^7 A cm^{-2} at near 0 K.

The critical current density is important in engineering because it limits the total current that can be passed through a superconducting wire or a device. The limits of superconductivity are therefore defined by the critical temperature T_c, critical magnetic field B_c (or B_{c2}), and critical current density J_c. These constitute a surface in a three-dimensional plot, as shown in Figure 8.52, which separates the superconducting state from the normal state. Any operating point (T_1, B_1, J_1) inside this surface is in the superconducting state. When the cuprate ceramic superconductors were first discovered, their J_c values were too low to allow immediate significant applications in engineering.

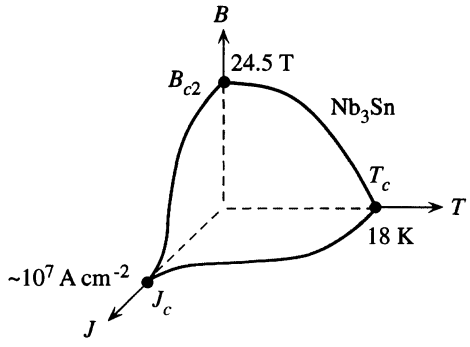

Figure 8.52 The critical surface for a niobium–tin alloy, which is a Type II superconductor.

Their synthesis over the last 10 years has advanced to a level that we can now benefit from large critical currents and fields. Over the same temperature range, ceramic cuprate superconductors now easily outperform the traditional superconductors. There are already a number of applications of these high-T_c superconductors in the commercial market.

EXAMPLE 8.8

SUPERCONDUCTING SOLENOIDS[9] Superconducting solenoid magnets can produce very large magnetic fields up to ~15 T or so, whereas the magnetic fields available from a ferromagnetic core solenoid is limited to ~2 T. High field magnets used in magnetic resonance imaging are based on superconducting solenoids wound using a superconducting wire. They are operated around 4 K with expensive liquid helium as the cryogen. These superconducting wires are typically Nb_3Sn or NbTi alloy filaments embedded in a copper matrix. A very large current, several hundred amperes, is passed through the solenoid winding to obtain the necessary high magnetic fields. There is, of course, no Joule heating once the current is flowing in the superconducting state. The main problem is the large forces and hence stresses in the coil due to large currents. Two wires carrying currents in the opposite direction repel each other, and the force is proportional to I^2. Thus the magnetic forces between the wires of the coil give rise to outward radial forces trying to "blow open" the solenoid, as depicted in Figure 8.53. The forces between neighboring wires are attractive and hence give rise to compressional forces squeezing the solenoid axially. The solenoid has to have a proper mechanical support structure around it to prevent mechanical fracture and failure due to large forces between the windings. The copper matrix serves as mechanical support to cushion against the stresses as well as a good thermal conductor in the event that superconductivity is inadvertently lost during operation.

Suppose that we have a superconducting solenoid that is 10 cm in diameter and 1 m in length and has 500 turns of Nb_3Sn wire, whose critical field B_c at 4.2 K (liquid He temperature) is about 20 T and critical current density J_c is 3×10^6 A cm^{-2}. What is the current necessary to set up a field of 5 T at the center of a solenoid? What is the approximate energy stored in the

---

[9] Designing a superconducting solenoid is by no means trivial, and the enthusiastic student is referred to a very readable description given by James D. Doss, *Engineer's Guide to High Temperature Superconductivity*, New York: John Wiley & Sons, 1989, ch. 4. Photographs and descriptions of catastrophic failure in high field solenoids can be found in an article by G. Broebinger, A. Passner, and J. Bevk, "Building World-Record Magnets" in *Scientific American*, June 1995, pp. 59–66.

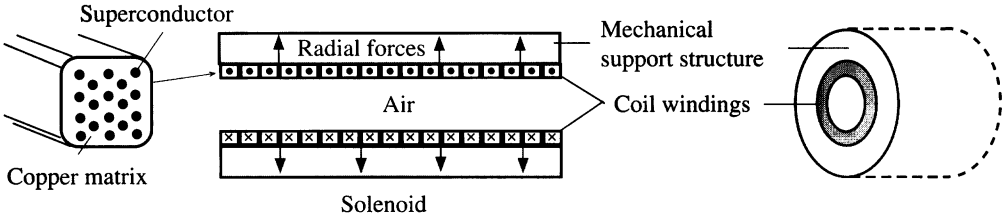

Figure 8.53 A solenoid carrying a current experiences radial forces pushing the coil apart and axial forces compressing the coil.

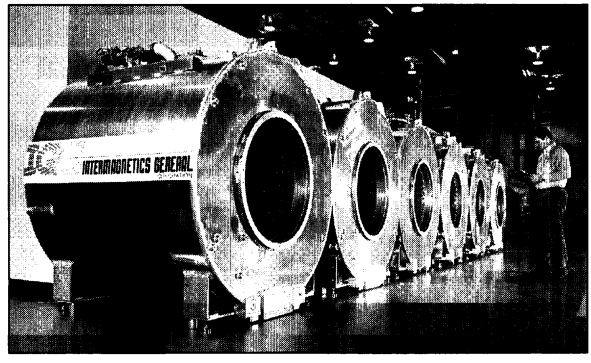

Superconducting electromagnets used on MRI. Operates with liquid He, providing a magnetic field 0.5–1.5 T.
SOURCE: Courtesy of IGC Magnet Business group.

solenoid? Assume that the critical current density decreases linearly with the applied field. Further, assume also that the field across the diameter of the solenoid is approximately uniform (field at the windings is the same as that at the center).

SOLUTION

We can assume that we have a long solenoid, that is, length (100 cm) $\gg$ diameter (10 cm). The field at the center of a long solenoid is given by

$$B = \frac{\mu_o N I}{\ell}$$

so the current necessary for $B = 5$ T is

$$I = \frac{B\ell}{\mu_o N} = \frac{(5)(1)}{(4\pi \times 10^{-7})(500)} = 7958 \text{ A} \quad \text{or} \quad 7.96 \text{ kA}$$

As the coil is 1 m and there are 500 turns, the coil wire radius must be 1 mm. If all the cross section of the wire were of superconducting medium, then the corresponding current density would be

$$J_{\text{wire}} = \frac{I}{\pi r^2} = \frac{7958}{\pi(0.001)^2} = 2.5 \times 10^9 \text{ A m}^{-2} \quad \text{or} \quad 2.5 \times 10^5 \text{ A cm}^{-2}$$

The actual current density through the superconductors will be greater than this as the wires are embedded in a metal matrix. Suppose that 20 percent by cross-sectional area (and hence as volume percentage) is the superconductor; then the actual current density through the

superconductor is

$$J_{\text{super}} = \frac{J_{\text{wire}}}{0.2} = 1.25 \times 10^6 \text{ A cm}^{-2}$$

We now need the critical current density J_c' at a field of 5 T. Assuming J_c decreases linearly with the applied field and vanishes when $B = B_c$, we can find J_c', from linear interpolation

$$J_c' = J_c \frac{B_c - B}{B_c} = (3 \times 10^6 \text{ A cm}^{-2}) \frac{20 \text{ T} - 5 \text{ T}}{20 \text{ T}} = 2.25 \times 10^6 \text{ A cm}^{-2}$$

The actual current density J_{super} through the superconductors is less than this critical value J_c'. We can assume that the superconducting solenoid will operate "safely" (with all other designs correctly implemented). It should be emphasized that accurate and reliable calculations will involve the actual J_c–B_c–T_c surface, as in Figure 8.52 for the given material.

Since the field in the solenoid is $B = 5$ T, assuming that this is uniform along the axis and the core is air, the energy density or energy per unit volume is

$$E_{\text{vol}} = \frac{B^2}{2\mu_o} = \frac{5^2}{2(4\pi \times 10^{-7})} = 9.95 \times 10^6 \text{ J m}^{-3}$$

so the total energy

$$E = E_{\text{vol}} \text{ [volume]} = (9.95 \times 10^6 \text{ J m}^{-3})[(1 \text{ m})(\pi 0.05^2 \text{ m}^2)]$$
$$= 7.81 \times 10^4 \text{ J} \quad \text{or} \quad 78.1 \text{ kJ}$$

If all this energy can be converted to electrical work, it would light a 100 W lamp for 13 min (and if converted to mechanical work, it could lift an 8 ton truck by 1 m).

8.10 SUPERCONDUCTIVITY ORIGIN

Although superconductivity was discovered in 1911, the understanding of its origin did not emerge until 1957 when Bardeen, Cooper, and Schrieffer formulated the theory (called the **BCS theory**) in terms of quantum mechanics. The quantum mechanical treatment is certainly beyond the scope of this book, but one can nonetheless grasp an intuitive understanding, as follows. The cardinal idea is that, at sufficiently low temperatures, two oppositely spinning and oppositely traveling electrons can attract each other indirectly through the deformation of the crystal lattice of positive metal ions. The idea is illustrated pictorially in Figure 8.54. The electron 1 distorts the lattice

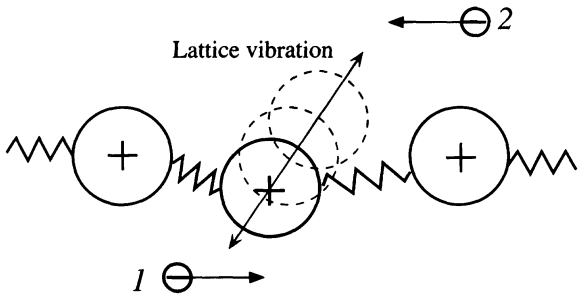

Figure 8.54 A pictorial and intuitive view of an indirect attraction between two oppositely traveling electrons via lattice distortion and vibration.

around it and changes its vibrations as it passes through this region. Random thermal vibrations of the lattice at low temperatures are not strong enough to randomize this induced lattice distortion and vibration. The vibrations of this distorted region now look differently to another electron, 2, passing by. This second electron feels a "net" attractive force due to the slight displacements of positive metal ions from their equilibrium positions. The two electrons interact indirectly through the deformations and vibrations of the lattice of positive ions. This indirect interaction at sufficiently low temperatures is able to overcome the mutual Coulombic repulsion between the electrons and hence bind the two electrons to each other. The two electrons are called a **Cooper pair.** The intuitive diagram in Figure 8.54, of course, does not even convey the intuition why the spins of the electrons should be opposite. The requirement of opposite spins comes from the formal quantum mechanical theory. The net spin of the Cooper pair is zero and their net linear momentum is also zero. There is a further significance to the pairing of electron spins in the Cooper pair. As a quasi-particle, or an entity, the Cooper pair has no net spin and hence the Cooper pairs do not obey the Fermi–Dirac statistics.[10] They can therefore all "condense" to the *lowest energy* state and possess one single wavefunction that can describe the whole collection of Cooper pairs. All the paired electrons are described collectively by a single coherent wavefunction Ψ, which extends over the whole sample. A crystal imperfection cannot simply scatter a single Cooper pair because all the pairs behave as a single entity—like a "huge molecule." Scattering one pair involves scattering all, which is simply not possible. An analogy may help. One can scatter an individual football player running on his own. But if all the team members got together and moved forward arm in arm as a rigid line, then the scattering of any one now is impossible, as the rest will hold him in the line and continue to move forward (don't forget, it's only an analogy!). Superconductivity is said to be a macroscopic manifestation of quantum mechanics. The BCS theory has had good success with traditional superconductors, but there seems to be some doubt about its applicability to the new high-T_c superconductors. There are a number of high-T_c superconductivity theories at present, and the interested student can easily find additional reading on the subject.

ADDITIONAL TOPICS

8.11 ENERGY BAND DIAGRAMS AND MAGNETISM

8.11.1 PAULI SPIN PARAMAGNETISM

Consider a paramagnetic metal such as sodium. The paramagnetism arises from the alignment of the spins of conduction electrons with the applied magnetic field. A conduction electron in a metal has an extended wave function and does not orbit any particular metal ion. The conduction electron's magnetic moment arises from the electron spin alone, and $\boldsymbol{\mu}_{\text{spin}}$ is in the opposite direction to the spin; $\boldsymbol{\mu}_{\text{spin}}$ can be either up

[10] In fact, the Cooper pair without a net spin behaves as if is were a **boson** particle.